2017

Dynamic Modeling of Thermal Management System with Exergy Based Optimization

Marcus J. Bracey
Wright State University

Dynamic Modeling of Thermal Management System with Exergy Based Optimization

A thesis submitted in partial fulfillment of the requirements for the degree of Master of Science in Mechanical Engineering

By:

Marcus J. Bracey
B.S.M.E., Wright State University, 2016

2017

Wright State University

WRIGHT STATE UNIVERSITY

GRADUATE SCHOOL

May 23, 2017

I HEREBY RECOMMEND THAT THE THESIS PREPARED UNDER MY SUPERVISION BY Marcus J. Bracey ENTITLED Dynamic Modeling of Aircraft Thermal Management System with Exergy Based Optimization BE ACCEPTED IN PARTIAL FULFILLMENT OF THE REQUIREMENTS FOR THE DEGREE OF Master of Science in Mechanical Engineering.

Committee on Final Examination

Rory Roberts, Ph.D

James Menart, Ph.D

Mitch Wolff, Ph.D

Robert E.W. Fyffe, Ph.D

Vice President for Research and
Dean of the Graduate School

Rory Roberts, Ph.D

Thesis Director

Mitch Wolff, Ph.D

Thesis Director

Joseph Slater, Ph.D, P.E.

Chair, Department of Mechanical
and Materials Engineering

ABSTRACT

Bracey, Marcus J., M.S.M.E. Department of Mechanical and Materials Engineering, Wright State University, 2016. Dynamic Modeling of Aircraft Thermal Management System with Exergy Based Optimization.

System optimization and design of aircraft is required to achieve many of the long term objectives for future aircraft platforms. To address the necessity for system optimization a vehicle-level aircraft model has been developed in a multidisciplinary modeling and simulation environment. Individual subsystem models developed exclusively in MATLAB-Simulink^{TM}, representing the vehicle dynamics, the propulsion, electrical power, and thermal systems, and their associated controllers, are combined to investigate the energy and thermal management issues of tactical air vehicle platforms. A thermal vehicle level tip-to-tail model allows conceptual design trade studies of various subsystems and can quantify performance gains across the aircraft. Often one of the main objectives is system efficiency for reduction in fuel use for a given mission. System efficiency can be quantified by either a 1st or 2nd law thermodynamic analysis. A 2nd law exergy analysis can provide a more robust means of accounting for all of the energy flows within and in between subsystems. These energy flows may be thermal, chemical, electrical, pneumatic, etc. Energy efficiency gains in the transient domain of the aircraft's operation provide untapped opportunities for innovation. To utilize a 2nd law analysis to quantify system efficiencies, an exergy analysis approach is taken. This work demonstrates the implementation of a transient exergy analysis for a thermal management subsystem component found on traditional aircraft platforms. The focus of this work is on the development of a dynamic air cycle machine (ACM) model and implementation of an

exergy based optimization analysis. This model is utilized in tandem with a bench top ACM experimental unit at the Air Force Research Laboratory's Modeling, Simulation, Analysis and Testing (MSAT) lab. Individual elements, including compressor, turbines, heat exchangers and control valves have been combined to investigate the behavior of a typical ACM. The experimental test stand is designed and constructed to be used as a method to validate models developed. Combining the results gained from the simulation studies, specifically the exergy analysis, and the experimental setup, a methodology is formulated for system level optimization. By leveraging this approach, future simulation studies can be implemented on various system architectures to generate accurate models and predictive analysis.

ACKNOWLEDGEMENTS

This work was completed under the guidance and direction of Drs. Rory Roberts and Mitch Wolff at Wright State University. I am grateful for the time they dedicated to this project, flexibility in working with my schedule, and most of all, the academic assistance they have provided as my research directors. In addition to their support, this work was supported by students and professionals to include Mark Bodie of AFRL, Dr. Jon Zumberge of AFRL, Sean Nuzum of Wright State, Adam Donovan of Wright State and the support from personnel located at the MSAT laboratory within Aerospace Systems Directorate at AFRL.

I also would like to thank my parents for the support they have provided throughout my academic career and providing me with the foundation for my academic success. Last but not least, I thank my wife, Michelle Bracey, for her understanding and unbounded support in all my academic pursuits.

Partial support for this project was supplied by the Dayton Area Graduate Studies Institute. The U.S. Government is authorized to reproduce and distribute reprints for Governmental purposes notwithstanding any copyright notation thereon. The views and conclusions contained herein are those of the authors and should not be interpreted as necessarily representing the official policies or endorsements, either expressed or implied, of Air Force Research Laboratory or the U.S. Government.

TABLE OF CONTENTS

TABLE OF FIGURES

LIST OF TABLES

NOMENCLATURE (TEXT)

ACM	=	Air Cycle Machine
AFRL	=	Air Force Research Laboratories
EDM	=	Exergy Destruction Minimization
EOA	=	Energy Optimized Aircraft
TMS	=	Thermal Management System
MEA	=	More Electric Aircraft
MIMO	=	Multiple Input/Multiple Output
M&S	=	Modeling and Simulation
ORC	=	Organic Rankine Cycle
VCC	=	Vapor Compression Cycle
WSU	=	Wright State University

NOMENCLATURE (EQUATIONS)

A	=	Valve Area
C_p	=	Specific Heat at Constant Pressure
C_{vf}	=	Specific Heat at Constant Volume of Fluid
C_{vw}	=	Specific Heat at Constant Volume of Volume Wall
D	=	Duct Diameter
e	=	Surface Roughness
E_{cv}	=	Control Volume Energy
eff	=	Heat Exchanger Effectiveness

f	=	Friction Factor
g	=	Gravitational Constant
h	=	Specific Enthalpy
k	=	Ratio of Specific Heats
L_{duct}	=	Duct Length
$\bar{M}_{avg}$	=	Average Molar Mass
m	=	Mass
m_v	=	Nodal Mass
m_{wall}	=	Mass of Volume Wall
$\dot{m}$	=	Mass Flow Rate
P	=	Pressure
P_{crit}	=	Critical Pressure
P_{ratio}	=	Pressure Ratio
Q_c	=	Cooling Work
Q_{heater}	=	Energy Added by Heater
$\dot{Q}$	=	Heat Transfer Rate
R	=	Ideal Gas Constant
R_u	=	Universal Gas Constant
t	=	Time
T	=	Temperature
S	=	Entropy
U	=	Internal Energy
v	=	Fluid Velocity

V	=	Volume
W_{net}	=	Net Work
$\dot{W}_{cv}$	=	Rate of Work on Control volume
$\dot{X}_{dest}$	=	Rate of Exergy Destruction
z	=	Potential Height
η	=	Efficiency
ρ	=	Density
μ	=	Fluid Viscosity
ψ	=	Specific Exergy Flow

1. INTRODUCTION

1.1. Problem Overview

Modern day aircraft are transforming as new technology and capabilities are integrated. As new capabilities are integrated, the behavior and overall requirements of the subsystems are altered. One such system that is transforming and becoming limited is the thermal management system (TMS) [1]. The 5^{th} generation aircraft are the first to operate with thermal deficits [2]. The 5^{th} generation aircraft have reduced ram air heat exchangers, fueldraulic actuators for thrust and nozzle area control and increased avionics and advanced electronics loads, which all increase the thermal loads on the aircraft.

The next generation aircraft is anticipated to have even higher low quality heat loads which would require a substantial amount of energy to remove the heat. The thermal and power loads are forecasted to increase by an order of magnitude for future aircraft platforms [3, 4]. The TMS must be capable of managing low temperature thermal loads on the aircraft. This is especially true as the advancement of aircraft move toward More Electric Aircraft (MEA). It is then crucial for the TMS design such that the heat load is managed efficiently to produce an Energy Optimized Aircraft (EOA). The TMS impacts the aircraft performance and interacts with the engine, fuel system and the electrical system. In order to properly assess the thermal demands aboard aircraft, research efforts exist to capture the dynamic behavior of these systems through the use of modeling and simulation (M&S). Through these models, the aircraft's capacity to complete a set of missions without sacrificing performance is better understood. While the models provide tactical insight into the behavior of the aircraft systems, the accuracy of the models must

be quantified. Validation testing must be performed to fully evaluate the aircraft systems and utilize the models. These modeling and validation efforts have evolved from the need to assess the power and thermal demands of current and future aircraft. To account for the energy conversions and losses, exergy analysis is incorporated to account for inefficiencies.

To understand the impact of increasing thermal management requirements, a full vehicle level analysis is needed. Vehicle-level analysis of subsystem interactions could result in significant performance gains across the aircraft, potentially improving the overall effectiveness of future platforms. The development of a vehicle level tip-to-tail (T2T) modeling and simulation tool would allow performance gains to be quantified in a cost effective manner. There are many types of energy being converted onboard the aircraft, chemical, pneumatic, mechanical, electrical and thermal. Therefore, consideration of the interaction between the various systems aboard the aircraft must be assessed. The interface between the thermal, power and electrical management systems is critical to capturing the dynamic behavior of the aircraft system as a whole. Utilizing the knowledge gained from the studies can provide the necessary information to optimize the performance of the aircraft throughout a mission. Recent work completed by Wright State University (WSU) and the Air Force Research Laboratory (AFRL) focused on the development of a non-proprietary, thermal T2T aircraft model in MATLAB-Simulink™ [5,6]. In addition, the non-proprietary nature of the model allows the tool to be distributed to various conceptual design groups and researchers. Specifically, it is foreseen that conceptual designers will use the model to conduct design trade studies, allowing the

analysis of multiple design configurations and the resulting subsystem interactions in short time periods [7-9].

1.2. Approach

AFRL has begun work to study different subsystems within aircraft thermal management system architectures, in an effort to accurately predict behavior using physics based models. One component that is incorporated in a typical TMS is an air cycle machine (ACM) [10,11]. The ACM mimics a traditional reverse Brayton cycle where air is ultimately cooled through use of turbomachinery. Air is compressed and then routed through a heat exchanger or series of heat exchangers before being expanded again by a turbine, which provides the mechanical work for the compressor. The current work involves the implementation of a physical test stand of an ACM that will be used to validate a Simulink model. In tandem with the development of a simulation model and bench top test stand, an exergy based analysis is used for system optimization and integration of the ACM into larger, more complex system models.

The modeling approach presented combines both energy and exergy principles based on the 1^{st} and 2^{nd} law of thermodynamics. Combining both these laws provides critical information that can be used for the design, operation, and improvement of systems across multiple platforms. In contrast, only utilizing the traditional 1^{st} law analysis can leave out important information about the system operation that can lead to an inefficient design [12, 13]. The exergy based approach used for the ACM is readily extensible to a systems-level assessment of a more complex TMS architecture model. By this, various subsystems are easily incorporated and integrated into large scale simulation models that include multiple energy domains and platforms such as that within a T2T model.

Simultaneously, the insights from the exergy analysis approach provide a basis for system level optimization, rather than component level. This is accomplished by using exergy destruction as a univariate metric for optimization [14]. Exergy destruction is specifically used because of the need to represent component losses in a consistent system level manner for the ACM model and future aircraft system models. The minimization of exergy destruction provides a single, consistent parameter for optimization across various subsystems within a large scale system level simulation. By developing a dynamic exergy analysis tool for the ACM, the transient behavior of the ACM is captured. The transient operation highlights where efficiency gains are that were previously untapped for optimization of an ACM. This is especially useful for studying conditions for a system to dynamically update control parameters for maximum achievable efficiency.

1.3. Thesis Organization

The thesis is organized as follows. Section 2 provides detailed background information pertaining to the ACM thermodynamic cycle and how it is implemented. Following this, the basis for an exergy based analysis is presented for the ACM system. Section 3 details the methodology used to develop the ACM model and bench top test stand. Although the bench top test stand is not studied in depth within this work, it is important to highlight the experimental side of this work as it provides information to the broad scope of the ACM project and how the ACM model was developed. Further, the derivation for the ACM model and exergy analysis is presented. An emphasis is placed on how to use exergy for optimization of the ACM operation. The method used to leverage the exergy analysis for optimal control of the ACM is presented. Section 4 provides the results of the

ACM study. The initial results of the ACM simulation based on the Simulink model are presented. The system optimization of the ACM based on exergy is shown through the dynamic control of the system. Section 5 summarizes the findings of the work performed and outlines key goals reached. Section 6 concludes the work and provides insight for the future work and next steps.

2. BACKGROUND

2.1. ACM Architecture

Aircraft thermal management plays a critical role in the performance and effectiveness of an aircraft during flight missions. Due to the high power demand of current aircraft platforms, the thermal loads experienced during operation have increased causing the aircraft TMS to handle higher heat loads than previously designed for. The effect of these high loads correlates to less efficient aircraft or can even cause failure to complete missions. The TMS aboard aircraft must be designed to handle the specified heat loads experienced throughout the mission. There are two different types of loads, high and low quality heat sources. The high quality sources have high enough temperatures to drive the heat to the heat sinks. The low quality heat sources have low temperature thermal energy that has to be pumped to higher temperatures via refrigeration systems to be dumped to the heat sinks. Electronic thermal loads such as avionics are low quality thermal sources which require refrigeration systems to transfer the thermal energy to the heat sinks. The refrigeration systems are typically reverse Brayton cycles with air as the working fluid, also known as air cycle machines (ACM). The air in a reverse Brayton cycle undergoes the following process in the ideal cycle through each state point. Process 1-2: Reversible,

adiabatic compression in a compressor. Process 2-3: Reversible, isobaric heat rejection in a heat exchanger. Process 3-4: Reversible, adiabatic expansion in a turbine. Process 4-1: Reversible, isobaric heat absorption in a heat exchanger. This process is shown in Figure 1 through a process flow diagram and T-S diagram.

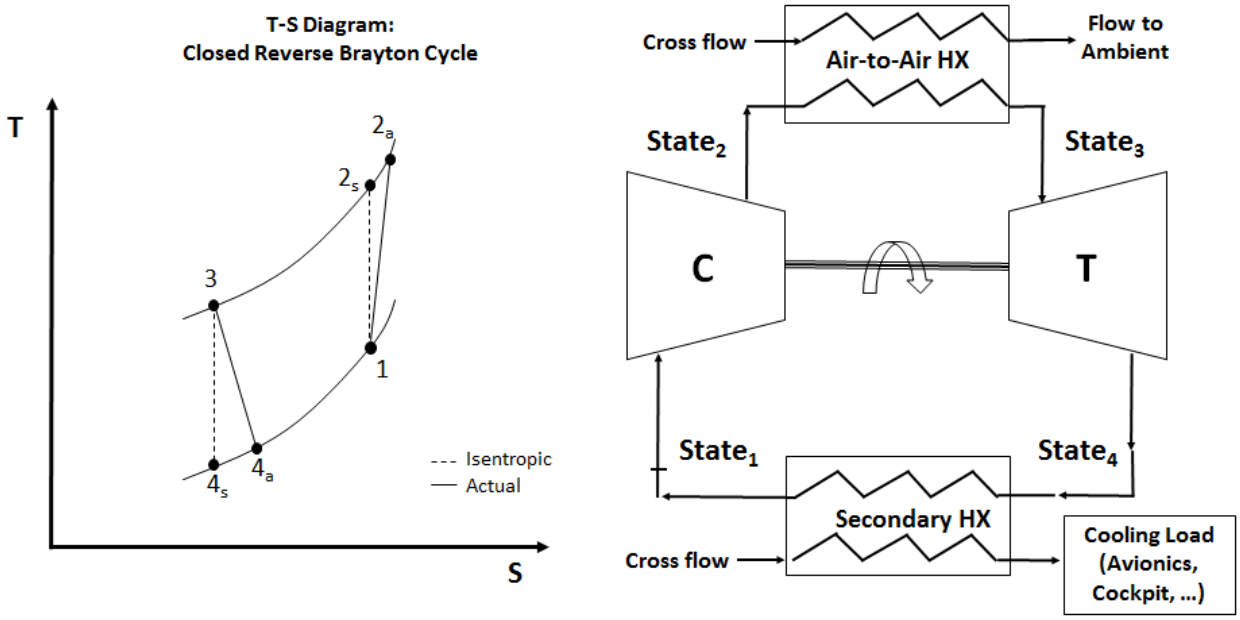

Figure 1. (Left) T-S diagram for closed cycle. (Right) Process flow diagram for closed cycle.

State points for closed Reverse Brayton cycle:

1) Compressor inlet

2s) Isentropic compression outlet

2a) Actual compression outlet

3) HX outlet

4s) Isentropic expansion outlet

4a) Actual expansion outlet

With the actual cycle, there are a few key differences that must be accounted for. The first being that the compression and expansion process is not isentropic, hence there is an exergy destruction rate associated with this process. Second, the pressure drop in the heat exchanger must be calculated to capture the losses other than the inherent losses in the heat exchanger effectiveness. This is the closed loop cycle form of the reverse Brayton cycle. For the model development, the open cycle is used where the inlet air is delivered through a reservoir and the exit air after the cooling turbine dumps into atmosphere. Having the open cycle eliminates the heat exchanger between state point 4 and 1. The open cycle process flow diagram is shown in Figure 2 as well as the state points on a T-S diagram.

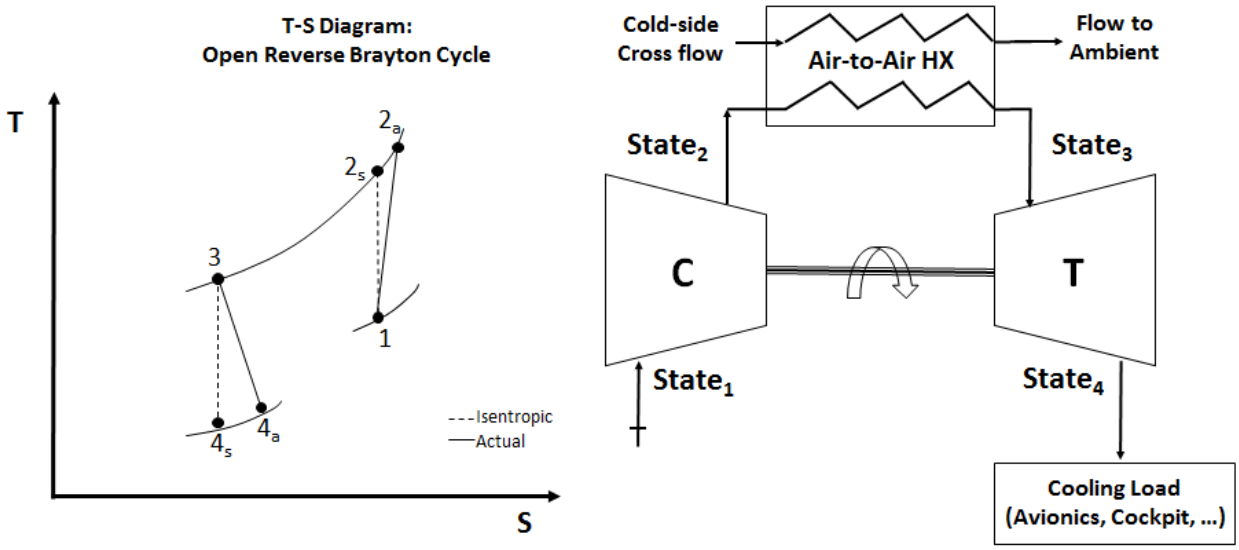

Figure 2. (Left) T-S diagram for open cycle. (Right) Process flow diagram for open cycle.

State points for open Reverse Brayton cycle:

1) Compressor inlet from reservoir

2s) Isentropic compression outlet

2a) Actual compression outlet

3) HX outlet

4s) Isentropic expansion outlet

4a) Actual expansion outlet to load

The open cycle provides various benefits to the closed cycle such as size and weight savings. This process was derived to closely mimic a two-wheeled or bootstrap cycle that is commonly found as an ACM unit on aircraft. The bootstrap cycle provides a significant increase in cycle efficiency compared to other ACM cycles. In the bootstrap ACM cycle, the compressor is used at the start of the process instead of a fan which is used in a simple ACM cycle. The bootstrap utilizes the power of the turbine to power the compressor. By providing an additional stage of compression at the beginning of the process, a higher efficiency can be achieved. However, the added heat of compression requires an additional heat exchanger between the compressor and turbine [15]. While the process shown in Figure 2 closely mimics the ACM setup used for this work, there are a few key states that are not shown. The final process flow diagram used for this work is shown in Figure 3. As shown, it is an open cycle that utilizes the basic structure of a bootstrap ACM cycle. The inlet air is taken from a shop supply and is modeled as a constant reservoir.

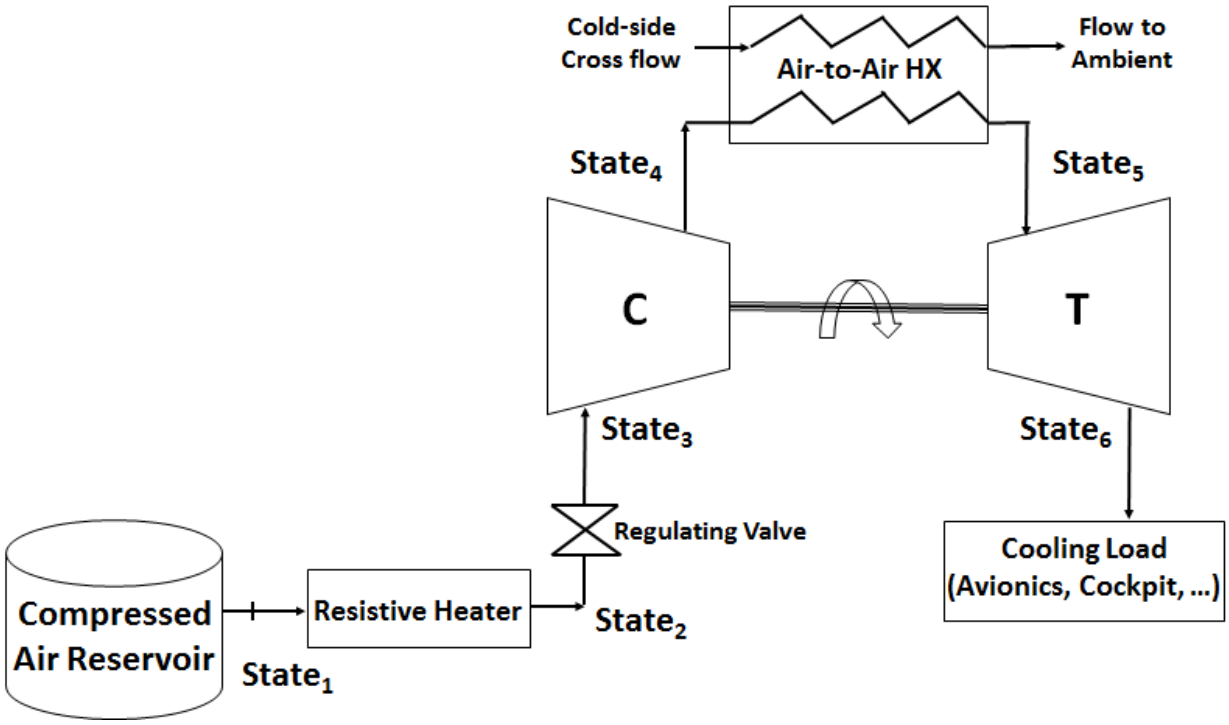

Figure 3. Process flow of the ACM cycle used for the model development.

This process is what was modeled for this work. The experimental setup up also follows this process except for the exit of the turbine at state 6 dumps to ambient. Future implementation of an experimental cooling load will be incorporated. The cooling load was modeled for the ACM simulation. This cooling load was used as a control constraint for operating the ACM to meet the cooling load demand. The components used in the final process that are not included in the other ACM cycles are the resistive heater and regulating valve. The heater is used to provide a constant heat flux to the air before it enters the compressor. This better simulates the boundary conditions experienced by a typical ACM unit aboard an aircraft. The pressure regulating valve allows for control of the ACM operating speed and cooling capacity. It does this by managing the flow of air from the reservoir and regulates the inlet pressure to the system. The air from the

reservoir is compressed at 100 psi/690 kPa and therefore must be managed to an appropriate pressure before entering the compressor. By appropriately controlling the regulating valve and heat load of the heater, the inlet pressure and temperature of the compressor are controlled and can be used to optimize the ACM performance. Each of these components were modeled and used in the experimental setup of the ACM. The process is further detailed on the T-S diagram of each state point. Figure 4 presents the T-S diagram for each state point along the ACM cycle used for this work.

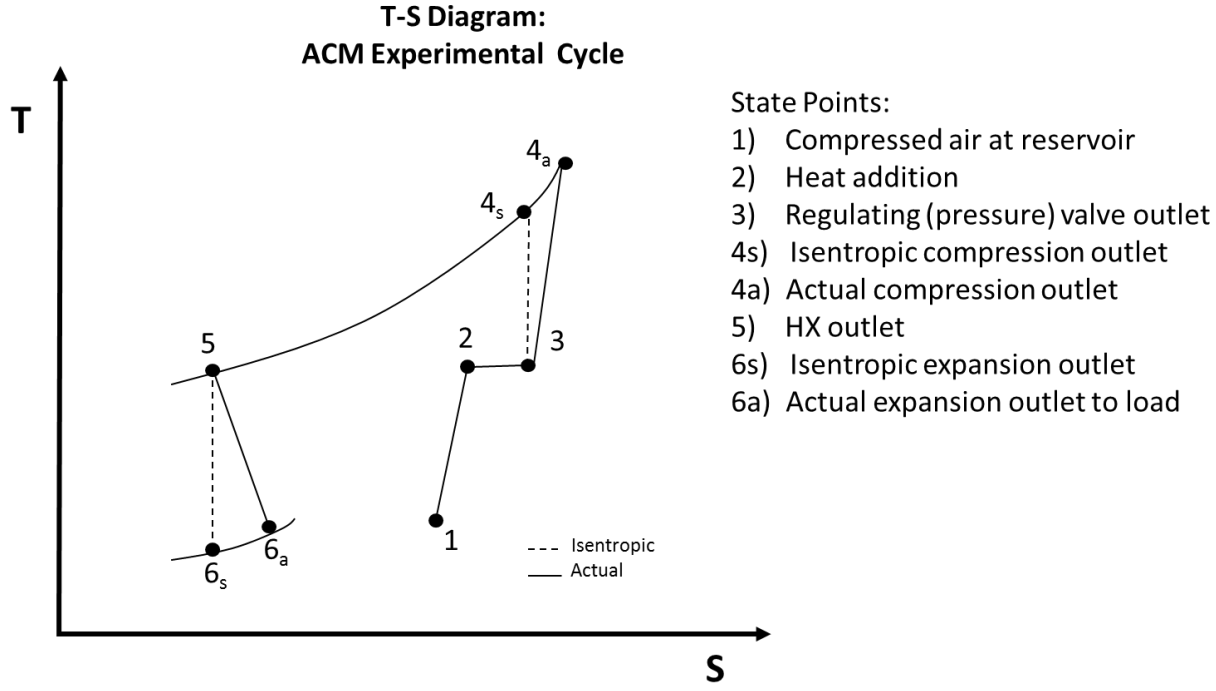

Figure 4. T-S diagram for final ACM process

When studying the air refrigeration cycle, it is important to define the operating performance or coefficient of performance (COP). The COP is given by,

$$COP = \frac{Qc}{Wnet} \quad (1)$$

where Q_c is the cooling capability and W_{net} is the total work provided to the ACM. The COP of an ACM is typically between 0.3 and 0.8 [13,14]. The ACMs are also driven by bleed air from the main engine, which have their own inefficiency associated with the compression of air in the main engine used to mechanically power the ACM. Assuming this conversion of pneumatic energy to work has efficiency of 30% and the COP is 0.4, the overall efficiency of removing low quality heat is 12%. It takes eight times the amount work to move the thermal energy from a cold temperature heat source to a hot heat sink. For example, a 10kW thermal load rate would require more than 80 kW work rate to transfer the heat to a higher temperature heat sink. Due to these inefficiencies, it is important to fully analyze the system performance, specifically the irreversibilities associated with the system. The COP provides a baseline performance parameter for the machine, but it fails to provide a detailed analysis of where the system is experiencing the majority of the lost work potential. For this, a system analysis must be performed which details where the system inefficiencies are most prevalent.

The current work on developing a simulation model of the ACM is complimented with the development of an exergy based analysis on the ACM. An exergy analysis is performed within the ACM model in order to better quantify the overall machine performance. The goal was to perform the exergy analysis of the system to better describe useful energy available to the ACM system. This will define the critical points of efficiencies within the machine as well as direct the power needs of the system as they relate to the overall thermal management system. With an exergy analysis, the design and

operation of components at the system level can be optimizing to reduce the irreversibilities within the system. Exergy destruction is particularly useful when looking at optimizing the system performance and obtaining a desirable operating point. Using the exergy based approach for system level analysis provides key benefits as opposed to traditional energy based analysis. First, the exergy destruction can be used as a common characterization for irreversibilities across multiple energy domains. This provides a baseline parameter to describe the efficiency of various components used within a larger system [18]. This is useful when analyzing complex systems with multiple components by virtue of a single metric to compare components against. Second, for each component within a system, the exergy destruction rate can be expressed as the sum of each component's exergy destruction. This allows for flexibility in the design and change of system components.

2.2. System Modeling

When studying large scale systems such as air or ground vehicles, power plants, or industrial processes, systems engineering can provide useful insight into the behavior of each component and system at large. Capturing the full behavior of the system and ensuring maximum efficiency at the system level poses many obstacles for the engineer to overcome. Griffin examined some common problems faced with systems engineering and capturing system interactions. He proposed a new perspective that focuses on design elegance [19]. This thought process of design elegance has brought forth many new and interesting viewpoints to tackle system level engineering and modeling. One popular answer for creating an elegant system is the utilization of the 2^{nd} law for thermodynamic analysis. The second law provides mathematical formulation to quantify the

irreversibility of a component, process or system. These irreversibilities are captured in an exergy analysis and can be applied to most systems engineering problems. Hence, exergy has been useful in many system level modeling and simulation efforts and has been used for the ACM efforts within AFRL and at WSU. Figure 5 presents a graphic describing the tiered approach to modeling and simulation of large scale systems.

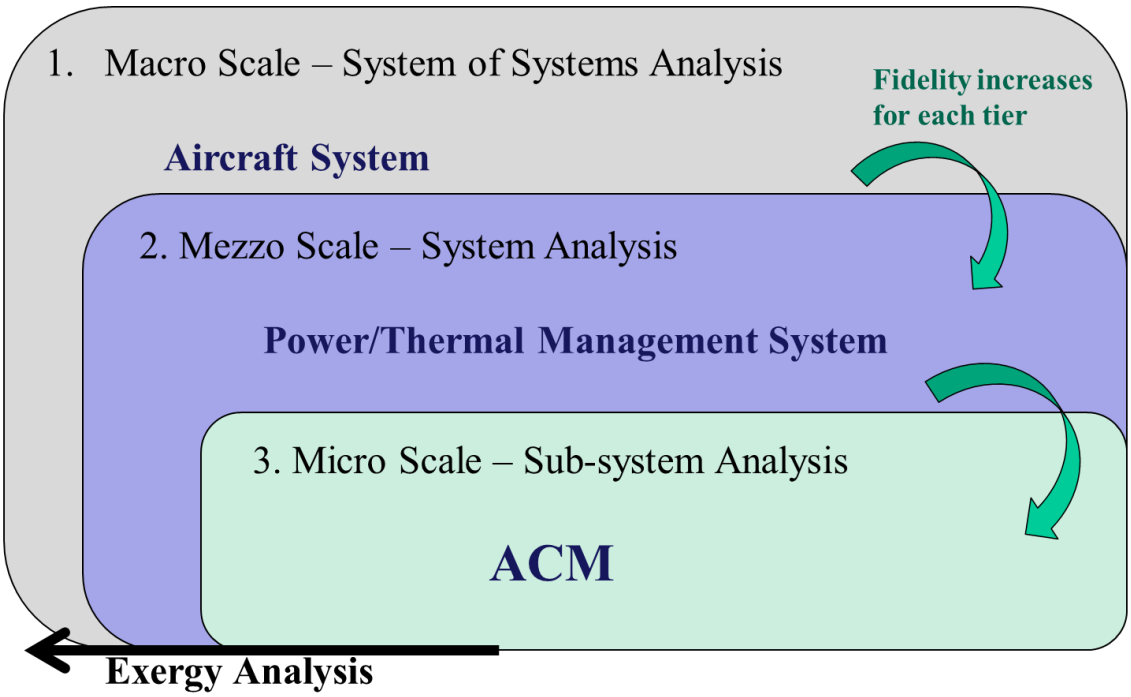

Figure 5. Tiered approach to modeling and simulation of large scale systems

As shown, to study a large scale system such as an aircraft, multiple tiers must be set up each with defined model fidelity. For this study, the ACM, a sub system of an aircraft thermal and power management system, was optimized. The fidelity of the ACM was much higher than a typical aircraft system model as larger scale systems require much more computational power to perform relatively small simulations. Exergy comes into play as a univariate approach to the multi-tier modeling approach. For a large scale

system of systems, exergy can be used as the answer to tying multiple sub systems together to gather an entire picture of the system operation.

Exergy, as a thermodynamic tool, can be used for many different applications such as design, optimization, and assessment of various engineering systems and components. Ahamed and others studied the method of using an exergy based analysis conducted on vapor-compression cycle (VCC) systems to determine the underlining effect of various parameters to improve the overall VCC system efficiency [20]. Similar work was done by Same, S. [21] where an organic Rankine cycle (ORC) was optimized based on the exergy analysis performed for various working fluids. The exergy analysis used in assessing the ORC power cycle was highly beneficial when studying the low quality waste heat of a typical power cycle as a power source for an ORC. Kim *et al.* [22] further investigated an ORC with an exergy analysis by studying the effect of turbine inlet pressure on the overall exergy destruction of the cycle. It is through an exergy analysis the research team was able to pinpoint the optimal inlet conditions for the turbine inlet. Other various studies have been conducted on the performance of turbo machinery and the use of exergy to detail their performance. Specifically, research on gas turbines in varied load conditions were investigated through exergy to detail the machine performance where an energy analysis would not be sufficient [22, 23]. Exergy has also been used as a performance criterion for experimental work in the thermodynamics field. Li *et al.* used an exergy analysis to characterize the performance of an adsorption cold thermal energy storage system [25]. The work detailed where the system inefficiencies were in an effort to predict the best operation on the proposed space cooling system.

In system level studies and analyses, exergy plays a crucial role in defining the system operating parameters and performance. Razmara *et al.* [26] outlined the method to use exergy-based predictive controls for the HVAC system in an industrial building. By this, operating conditions were chosen for peak performance when needed. Similarly, performing an exergy analysis can provide knowledge to the theoretical upper limit of the system performance as seen in [27]. Exergy has proven to be useful in many different applications, but it has been shown to be specifically beneficial in system level studies where multiple components are at play. For this work, an exergy analysis similar to the ones mentioned above is utilized to capture the transient behavior of the ACM and highlight the optimal control conditions during operation.

2.2.1. Exergy Analysis Formulation

Utilizing the first law of thermodynamics to perform an energy based analysis for a thermodynamic system can provide useful insight into the behavior of the system. Mathematically, the first law is written as the conservation of energy equation given by,

$$\frac{dEcv}{dt} = \dot{Q}_{cv} + \dot{W}_{cv} + \dot{m}_i(h_i + \frac{v_i^2}{2} + gz_i) - \dot{m}_e(h_e + \frac{v_e^2}{2} + gz_e) \qquad (2)$$

where *cv* represents the control volume, *i* represents inlet state, and *e* represents the exit state.

However, performing such an analysis is limited. By adding a second law perspective into the analysis, a full description of the thermodynamic system can be achieved. The second law introduces the irreversibility of the system by means of entropy. Another method commonly used to study the irreversibility of a process or system is to study the exergy. Exergy is defined as the maximum reversible work that a system can deliver from

an initial state to the state of the surrounding environment [28]. Mathematically, the flow stream exergy transport,ψ, through a control volume is defined as,

$$\psi = (h - h_0) - T(s - s_0) + \frac{v^2}{2} + gz \tag{3}$$

where T_0, h_0, and s_0 are the temperature, specific enthalpy, and specific entropy of the reference or dead state environment. For a given control volume, thermo-mechanical exergy can be transferred in three different methods: heat transfer, work transfer, or mass transfer. The exergy balance in rate form for a control volume is given by,

$$\frac{dXcv}{dt} = (1 - \frac{T_0}{T})\dot{Q}_{cv} - (\dot{W}_{cv} - P_0 \frac{dV_{cv}}{dt}) + \dot{m}_i(\psi_i) - \dot{m}_e(\psi_e) - \dot{X}_{dest} \tag{4}$$

where P_0 is the reference pressure, $\dot{W}_{cv}$ is rate of work across the boundary, and $\dot{Q}_{cv}$ is the rate of heat transfer across the boundary. Exergy, unlike energy, is not always conserved. The second law establishes the increase of entropy principle which can be restated using exergy. Exergy must always decreases for an irreversible process. This gives rise to a quantitative measure of the irreversibility of a system, exergy destruction. Exergy destruction is defined as

$$\dot{X}_{dest} = T_0 \dot{S}_{gen} \geq 0 \tag{5}$$

Note that for actual processes, the exergy destruction is positive, whereas for a reversible process, the exergy destruction is zero.

Exergy destruction is useful in determining the optimal performance of a system. Exergy analyses based on this formulation have been used extensively to understand system level component interactions and can pinpoint the largest source of irreversibility in the overall

system. Specifically, the minimization of exergy destruction throughout components has been used in many system level optimization problems. Utilizing this analysis, design changes can be made at the component level to improve the system performance [18]. One such example of using an exergy analysis at the design level was to optimized the heat exchanger used in aircraft environmental control systems [29].

2.2.1.1. Exergy Destruction Minimization

Using the thermodynamic optimization approach, exergy destruction minimization (EDM), has proven to be a useful method to system level optimization. One reason for this is that EDM provides a univariate approach across various energy platforms. Because exergy destruction is a common metric, it allows for a direct comparison between multiple subsystems. For the ACM in study, an operating metric for efficiency commonly used is the COP. This provides useful insight into how the specific ACM subsystem is operating. However, other systems within an aircraft are characterized by additional parameters such as fuel consumption for the aircraft engine. This difference in defining a common parameter is problematic for large system level analyses. Using exergy destruction as the common metric across multiple domains provides an elegant solution to this problem.

2.2.1.2. Exergy Minimization Control

Exergy destruction provides an objective function for optimal control of systems. Different methods have been used to implement an EDM controller for thermodynamic optimization. One approach that has seen significant research over the past decade is utilizing model predictive control with exergy as a cost function. Model Predictive Control (MPC) predicts and optimizes time-varying processes over a future time horizon.

MPC is useful for MIMO plants where the demands of the plant are well known. For a transient simulation, MPC is used to provide real time control of a system in an effort to optimize the system operation. Jain was able to use exergy destruction as the objective function in the control of an integrated energy system [30]. The work implemented an exergy based MPC approach with the goal to achieve maximum efficiency while meeting the demand of the energy system. Hadian and Salahshoor used exergy losses as the criterion to analyze a MIMO industrial process [31, 32]. By performing an exergy based analysis, information was gained as to where the processes that consumed the majority of exergy were. The process was optimized with MPC by reducing the exergy losses through improving control performance. While MPC provides many benefits for control systems, the intense computational demands limit the actual utilization in environments where the computing platform is constrained. For this work, a method for optimal control is developed based on exergy destruction that can be readily employed without introducing additional computational burden. By using a rigorous study of basic PI controllers and gain scheduling, the optimal control of the ACM is studied through simulation for many various different environments.

3. METHODOLOGY

To develop the ACM bench top experimental unit and the corresponding Simulink model, automotive components for the ACM were selected for the turbomachinery and heat exchanger. By employing automotive turbochargers, a bootstrap ACM architecture can be designed which mimics traditional ACM's found on multiple aircrafts. The bootstrap system has a compressor, turbine, HX, valves, and ducting like that of an ACM

implemented in actual aircraft. By validating the component models with the experimental bench top unit, these component models can then be used in the construction of future system model architectures. The methodology generated through this work can then be exploited for the development of a more accurate modeling approach.

3.1. Air Cycle Machine Description

The transient ACM model developed in the MATLAB-Simulink^{TM} environment is modeled after the physical bench top test setup of an ACM. The ACM simulation model will be used in tandem with the bench top setup of the ACM. This allows for validation of the model in order to assess the accuracy of the model. The ACM model and bench top test unit both use a series of controllers for various inputs to the system that control the ACM system performance.

Inputs and boundary conditions for the ACM model include: 1) inlet air temperature, pressure, and humidity; 2) fan air temperature, pressure, and mass flow; 3) ambient temperature, pressure, and humidity; 4) regulating valve control pressure; and 5) heater load. The majority of these boundary conditions can be controlled and/or measured through a series of controls/sensors giving the ACM model the flexibility needed for experimental validation. Upon running the model, outputs are the station point temperature, pressures, and mass flows before and after each main component in the ACM.

Within the model, each key component of the ACM is included. The whole ACM system is divided into subsystems that describe the individual components as well as the ducting

before and after each component. The first subsystem is the heater. This heater is used to indirectly control the temperature of the flow entering the compressor. The next subsystem is the regulating valve, which is connected to the heater by another duct system. The regulating valve is composed of three sections, input and output nodes and the valve itself. This is the critical control device for the system that regulates the inlet pressure to the compressor. The next block is the compressor and turbine combination. Unlike the previous subsystems, this one is controlled by performance maps. These maps were numerically generated with the knowledge of the geometry and design through turbomachinery design software. Between the compressor and turbine is a heat exchanger. The heat exchanger has four components that are modeled. It has an inlet flow chamber for the hot air coming from the compressor, an outlet flow chamber for the hot air traveling to the turbine, an inlet flow chamber for the cold crossflow, and an outlet flow chamber for the cold crossflow. Both of the inlet and outlet blocks for the hot air function similarly. For the cross flow, a fan with constant flow rate will be used as the cooling medium within the heat exchanger.

3.2. Bench Top Test Unit

When performing M&S studies, it is important to gain an understanding of how accurately the model predicts the behavior of the system. Due to the limited scope of this work, experimental data for an exergy analysis has yet to be completed. Because the model was developed from the experimental unit, the description of the bench top unit is outlined in the following sections. Future work will look to study how to properly investigate and validate the ACM simulation exergy analysis to experimental results.

3.2.1. Experimental Setup

At its core, a Garrett 1548 turbocharger is used with a Vibrant Performance 12616 intercooler as the heat exchanger. A medium sized fan is used to move ambient air through the cold side of the heat exchanger. The fan was sized to meet the demands of the system and is estimated to provide up to 60 lbs/min (0.45 kg/s) of airflow through the heat exchanger. This flow rate ensures that the heat exchanger effectiveness is high enough that the temperature to the turbine inlet is at a reasonable point.

In general this system architecture has three main controllable inputs to determine the performance. The first is the amount of heat applied to the pressurized air supply before entering the inlet of the compressor. This heat load serves as a disturbance to the system that is controlled to manage the temperature of the air at the compressor inlet. Second, the regulating valve controls the inlet flow pressure to the compressor. The pressure is limited to between 20 psia / 137 kPa and 45 psi / 310 kPa. These values come from analyzing the compressor efficiency based on the compressor maps. This is an important control variable because it plays a large role in the operating speed of the turbomachinery and overall performance. Last, the fan flow rate across the cold side of the heat exchanger is controlled. The fan flow across the heat exchanger represents the bypass air across a typical ACM heat exchanger. For a typical mission, this airflow varies over the course of a mission. The CFM output of the fan will determine the effectiveness of the heat exchanger.

3.2.2. Process and Flow Diagram

There are variables that cannot be controlled throughout a test. The air from the in-house air supply has temperature and pressure that vary as the in-house air supply cannot be

controlled. Sensors will measure these parameters on the physical system and will be adjusted in the model to mimic the testing conditions. In addition to these sensors measuring the air supply, a series of other sensors will be used to collect the data during operation. Figure 6 provides a schematic of the system architecture as well as the station points where sensors will be located to collect the desired data.

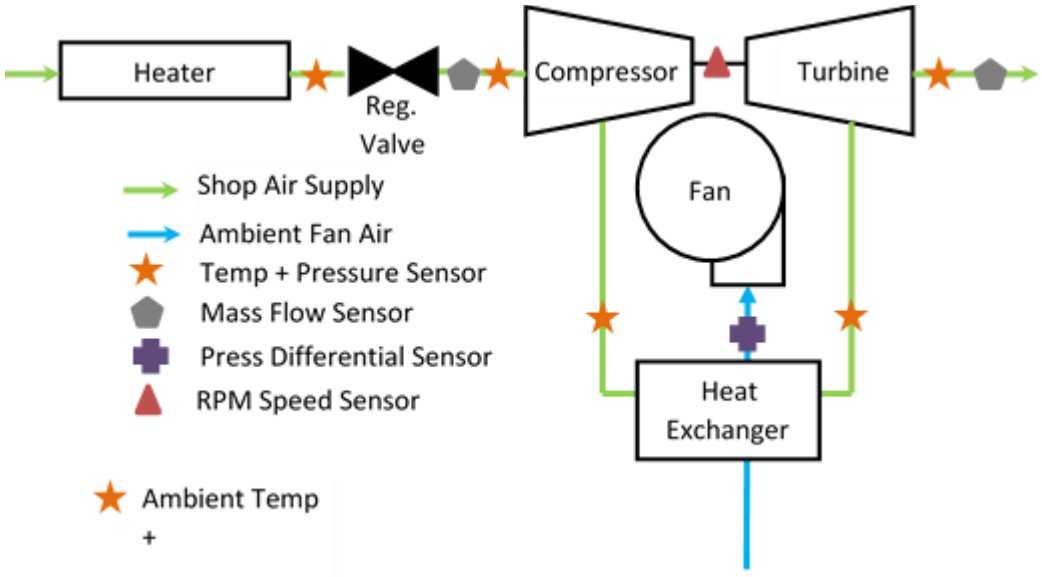

Figure 6. ACM test stand process and instrumentation diagram (P&ID)

For outputs from the experiment, there are several places where data is taken that can be compared later to the model. This requires a flexible model that is easily adjusted to match the experimental conditions. The experimental design allows for temperature and pressure readings at many points along the air flow. These two parameters are measured before and after each of the major components. Additionally, the mass flow is measured in the hot flow after the regulating valve. The mass flow is also measured from the fan on the cold air flow using a pressure differential sensor. The speed of the turbocharger is

measured at the shaft connecting the two. Through collection of data, the test stand will provide crucial data to validate the ACM model.

3.2.3. ACM Component Selection

The components used in both the model and the experimental bench top test stand were chosen based on various parameters. The physical test stand of the ACM incorporates readily available parts whose information is easily obtained. The decision was made to design and build the ACM from automotive parts including a turbocharger for the turbine and compressor and an intercooler for the heat exchanger. The machine specifications for each of the parts used are easily obtained to fully define the system in the model. The core components of the ACM are the turbine, compressor, and heat exchanger. The model development of the ACM requires detailed performance maps for the turbo-machinery and heat exchanger. The first step in generating the turbo-machinery maps was to select the appropriate turbo-machinery. The sections below describe the turbo-machinery selection process as well as the development of the compressor and turbine performance maps. The heat exchanger was then sized according to the demands of the turbomachinery selected. The heat exchanger selected had to be large enough to provide enough heat transfer between the turbine and compressor such that the turbomachinery would be operating at the highest efficiency. A heat exchanger sizing routine was developed to generate initial performance maps for the ACM heat exchanger. The heat exchanger performance map was generated based on the size, surface treatment, geometry, and material.

Turbomachinery

ACM's used in automotive applications closely mimic those used in the aerospace industry. Both have a centrifugal compressor and turbine, but the air stream conditions entering each component, compressor and turbine, are much different in the automotive application when compared to the aerospace ACM application. In the automotive application, the compressor inlet air stream is at ambient pressure and temperature conditions while the turbine accepts hot exhaust gases in the range of 1500^{o}F / 816^{o}C or more. In the bootstrap ACM application, the compressor inlet air stream conditions are at elevated pressures and temperatures, and the turbine inlet conditions are at lower temperatures, in the range of 120^{o}F / 50^{o}C. These large differences in compressor and turbine inlet conditions, between the automotive and aerospace ACM application, can result in improper compressor and turbine matching.

In order to minimize compressor and turbine matching issues, research was completed to identify the most appropriate turbocharger for the aerospace ACM application from readily available turbochargers in the market. The turbochargers were selected by matching the actual mass flow of the compressor and turbine with inlet boundary conditions of 25psia/172 kPa and 200^{o}F/94^{o}C for the compressor and 50psia/345 kPa and 120^{o}F/50^{o}C for the turbine. These are the boundary conditions of the compressor and turbine that the ACM bench tests were designed to handle. Through basic turbocharger research, the manufacturer chosen was Garret by Honeywell [33]. The company provided compressor and turbine maps for each turbocharger based on the corrected compressor mass flow. Garret provides over 80 different turbochargers that could be used for this system. In order to narrow the selection to one, the performance maps of the

turbochargers were analyzed. The needed corrected mass flow was determined for the operating boundary conditions and the actual mass flow was determined, by

$$\dot{m}_a = \dot{m}_c \frac{{}^{P_a}/_{14.7psia}}{\sqrt{{}^{T_a}/_{519\ R}}} \quad (6)$$

where m_a is the actual mass flow (ppm), m_c is the corrected mass determined from the compressor map (ppm), P_a is the inlet compressor pressure (psia), and T_a is the inlet compressor temperature (R). The actual mass flow is determined from the above equation and compared to that of the turbine. Using the turbine maps at a constant pressure ratio, the corrected turbine mass flow is determined. For a perfectly matched system, the ratio of the turbine and compressor corrected mass flow would be 1. After this analysis, the GT1548 turbocharger provided the best match for the demands of the ACM bench top test stand.

In addition, to the compressor to turbine mass flow matching, the ACM test bench mass flow must be compatible with the available heater and facility air. The 25kW heater used to preheat the house air has the ability to increase the facility air temperature to the 200^{o}F / 94^{o}C required by the compressor. The compressor mass flow requirement is also well below the facility air capability of 180 pounds per minute (ppm) / 1.36 kilograms per second (kg/s) at 100psia / 690 kPa. Because of the compressor and turbine mass flow matching and mass flow capability with the facility air and existing heater, the GT1548 was selected for the ACM test bench turbo-machinery.

To accurately model the ACM system, performance maps were generated for the compressor and cooling turbine. These maps were numerically generated with the knowledge of ACM geometries and design by means of turbomachinery software package. These performance maps are implemented in the ACM model and include calculations based on mass flow, pressure ratio, shaft speed, and efficiency.

ConceptsNREC [34] is a company that offers software packages that calculate the necessary performance characteristics of radial turbines and compressors. The software packages output the performance map characteristics with all geometry and design considerations taken into account. This allows us to export the performance maps from the software and include in the overall model. The maps created were developed on a trial basis of the ConceptsNREC software COMPAL and RITAL.

3.3. ACM Model Development

In this work, all modeling efforts were done in the MATLAB-Simulink^{TM} environment. The ACM model is developed without iteration loops (algebraic constraints) and all states are continuous. This approach is very important for complex system level simulations of stiff dynamic systems. By modeling all the significant states as continuous states and not steady-state approximations with discontinuities, advanced numerical solvers for stiff systems may be used. Numerical solvers for stiff systems rely on the Jacobian matrix and thus require accurate approximations for gradients of all continuous states. The following sections provide a detailed description of the modeling approach for the transient ACM model.

For the ACM model, a nodal volume approach was taken to model the flow between system components. This approach includes three main elements being modeled; 1) A flow resistive element which represents the ducting, 2) Nodal volumes before and after system components, 3) System components such as regulating valve, turbine, compressor, etc. The mass continuity and energy balance equations were applied to nodal volumes both before and after major components, generating nodal pressure and temperature states. Flow resistance equations based on ducted flow were used between nodal states to determine the mass flow between nodes. The nodal volumes inputs are based on the resistive flow calculations from the ducting and boundary conditions. The Swamee and Jain correlation is used to determine the duct mass flow [35].

$$\dot{m} = \left(\rho(-0.965)\sqrt{\frac{\Delta P * D^5}{\rho L}}\right)\left[log\left(\left(\frac{e}{3.7D}\right) + \frac{\sqrt{3.17 * \left(\frac{\mu}{\rho}\right)^2 L\rho}}{\Delta P * D^3}\right)\right] \tag{7}$$

where $\dot{m}$ is the fluid mass flow, ρ is the fluid density, ΔP is the differential in pressure, D is the duct diameter, L is the duct length, e is the surface roughness, and μ is the fluid viscosity. The direction of the mass flow through the resistive ducting elements is determined by the differential in pressure across the element. The differential in pressure is based on the difference in the nodal volume pressure after the duct and the boundary conditions at the duct inlet. This method requires an initial nodal pressure that represents the initial pressure within the system components. The fluid mass within each nodal volume is determined from the mass continuity shown below,

$$\int dm_V = \int (\dot{m}_i - \dot{m}_o)dt \tag{8}$$

where m_i is the mass flow entering the nodal volume, m_o is the mass flow exiting the nodal volume, and m_V is the nodal mass.

The energy conservation equation is used to determine fluid nodal temperature shown below,

$$\frac{d(m_V u_V)}{dt} = \dot{m}_i h_i - \dot{m}_o h_o \tag{9}$$

where h_i is the inlet stream enthalpy, h_o is the outlet stream enthalpy, and u_v is the nodal volume internal energy. By incorporating the volume wall thermal capacitance into (9), the energy equation becomes

$$\frac{d(m_V)}{dt} u_V + \left(m_V C_{Vf} + m_w C_{Vw}\right) \frac{\mathrm{dT}}{\mathrm{dt}} = \dot{m}_i h_i - \dot{m}_o h_o \tag{10}$$

$$\frac{dT}{dt} = \frac{(\dot{m}_i h_i - \dot{m}_o h_o - \frac{d(m_V)}{dt} u_V)}{(m_V C_{Vf} + m_w C_{Vw})} \tag{11}$$

where *Cvf* is the specific heat at constant volume of the fluid, m_w is the wall mass, *Cvw* is the specific heat of the wall and *T* is the temperature of the element. The pressure at the node is found through the use of the ideal gas law shown,

$$\rho = {}^{m}/_{V} \tag{12}$$

$$P = \rho RT \tag{13}$$

where V is the nodal volume, R is the ideal gas constant, T is the nodal temperature, and P is the nodal pressure.

3.3.1. System Components

The ACM model revolves around modeling five core components. These are the heater, regulating valve, turbine, heat exchanger, and compressor. As mentioned, the ducting between each system elements was modeled as a resistive flow element. The basic derivation for each system model is described in the following sections.

Heater

The first subsystem is the heater. This heater is used to indirectly control the temperature of the flow entering the compressor. This acts as a disturbance to the system and will have a large impact on the exergy destruction and overall performance of the ACM. The conservation of mass for this system is shown in the following equation.

$$m = \int \dot{m}_{in} - \dot{m}_{out} dt \tag{14}$$

With the mass accumulated in the system, the pressure can be found using ideal gas law in the following equation.

$$P = \frac{mRT}{V} \tag{15}$$

The temperature after the heater element is found by the energy equation.

$$\frac{dT}{dt} = \frac{Q_{heater} + \dot{m}h_{in} - \dot{m}h_{out} - \frac{d(m_v)}{dt}U}{m_v C_{vf} + m_{wall} C_{vw}} \tag{16}$$

The Q_{heater} represents the energy that the heater delivers to the airflow. The enthalpy terms are calculated using relationships with temperature for dry air and then the flow rate.

The heater acts as a heat load on the incoming air into the ACM. This heat load is representative of the heat of compression from the main engine compressor. By controlling the amount of heat input, the ACM can be run through various cycles that simulate different operating conditions and environments for the ACM. Thus, the amount of heat input into the air before entering the ACM is defined as a critical control parameter for operation of the ACM.

Regulating Valve

The next subsystem is the regulating valve, which is connected to the heater by another duct system. The regulating valve is composed of three sections, input and output nodes and the valve itself. The input and output nodes are identical. They operate in a similar manner to the heater with the following equation set finding the accumulated mass in the system using conservation of mass and ideal gas equation to find the pressure. This element is the main control element for the ACM model. The inlet pressure which is determined by the valve directly affects the operating conditions for the ACM.

The modulating valve is modeled as an ideal gas, one-dimensional, steady, frictionless, and adiabatic flow through a converging nozzle. The valve area is determined by a feedback control system that compares the desired pressure to the pressure on the outlet node. The mass flow is calculated using,

$$\dot{m} = A\sqrt{\left(\frac{2k}{k-1}\right)(P_{max})(\rho)\left(P_{ratio}^{\left(\frac{2}{k}\right)} - P_{ratio}^{\frac{(k+1)}{k}}\right)} \tag{17}$$

The regulating valve is the key component that is used as a control parameter for the ACM. By regulating, the inlet pressure, the operating conditions of the ACM are determined. The pressure after the regulating valve is defined as a critical control parameter for operation of the ACM like the heat input.

Turbine/Compressor

The compressor and turbine model used in this effort determines the outlet pressure, temperature, and power given shaft speed and inlet pressure and temperature. The power generated by the turbine is matched to the power consumed by the compressor. The compressor and turbine models use performance maps which relate pressure ratio, corrected mass flow, corrected speed, and efficiency.

The corrected mass flow associated with the compressor and turbine is calculated by,

$$\dot{m}_c = \dot{m}\,\frac{\sqrt{T_i/T_{std}}}{P_i/P_{std}} \tag{18}$$

where $\dot{m}_c$is the corrected mass flow, $\dot{m}$ is the actual compressor mass flow, T_i is the compressor inlet temperature, T_{std} is standard temperature, 519^{o}R, P_i is the compressor inlet pressure, and P_{std} is standard pressure, 14.7 psi. The corrected speed is given by

$$N_c = \frac{N}{\sqrt{T_i/T_{std}}\, P_i/P_{std}} \tag{19}$$

where N is the actual speed and Nc is the corrected speed.

The compressor and turbine models use variable specific heat methodology to determine the outlet temperature and power. This is done by calculating the change in entropy to determine isentropic efficiency. The ideal gas entropy change is given by,

$$s_2 - s_1 = \int_1^2 C_p\,(T)\,\frac{dT}{T} + R ln \frac{P_2}{P_1} \tag{20}$$

where T is the flow temperature, R is the ideal gas constant, P_2 is the outlet pressure, P_1 is the inlet pressure, s_2 is the outlet entropy, s_1 is the inlet entropy, and $C_p(T)$ is the specific heat based as a function of temperature. To find the entropy property at the given temperature, the entropy air property is found using,

$$s^o = \int_0^T C_p\,(T)\,\frac{dT}{T} \tag{21}$$

The outlet isentropic entropy is found along with the compressor inlet pressure, inlet temperature, outlet pressure along with the s^o air property. With the outlet isentropic entropy known, s^o is used to calculate the isentropic exit temperature.

For the compressor, the actual outlet temperature is determined by first calculating the compressor inlet and isentropic outlet enthalpy along with the compressor efficiency, or

$$H_2 = \frac{(H_{2s} - H_1)}{eff} + H_1 \tag{22}$$

where H_2 is the actual compressor outlet enthalpy, H_{2s} is the isentropic compressor enthalpy, H_1 is actual compressor inlet enthalpy, and *eff* is the compressor efficiency. The outlet enthalpy is used to determine the actual compressor outlet temperature. Finally, the compressor power is determined by,

$$P_c = \dot{m}(H_2 - H_1) \tag{23}$$

For the turbine, the actual outlet enthalpy is found by,

$$H_4 = H_3 - (H_3 - H_{4s})eff \tag{24}$$

where H_4 is the actual turbine outlet enthalpy, H_{4s} is the isentropic turbine enthalpy, H_3 is actual turbine inlet enthalpy, and *eff* is the turbine efficiency. The outlet enthalpy is used to determine the actual compressor outlet temperature. The power delivered by the turbine is determined by,

$$P_t = \dot{m}(H_3 - H_4) \tag{25}$$

Based on these equations, the outputs of the turbine and compressor are given. The actual outlet mass flow and outlet temperature are output to a nodal element which determines the outlet pressure and temperature.

Heat Exchanger

The ACM heat exchanger is used to reject heat from the compressor outlet air stream to the environment before entering the turbine. The HX model employs effectiveness and pressure drop maps based on test data and performance prediction methods taken from Kays and London [36]. This method is easily incorporated into the ACM model.

The heat exchanger has four nodal volumes used to model the flow through both the hot and cold side. It has an inlet flow chamber for the hot air coming from the compressor, an outlet flow chamber for the hot air traveling to the turbine, inlet chamber for cold air stream from the fan, and an outlet chamber for cold air exiting the heat exchanger. Both of the inlet and outlet blocks for the hot air function similarly.

The $Q_{heat\ transfer}$ in the heat exchanger is calculated by,

$$Q_{heat\ transfer} = eff\left(\dot{m}_{hot\ out}\ C_{p\ hot}(T_{hot\ in} - T_{cold\ in})\right) \tag{26}$$

where $C_{p\ hot}$ is the specific heat for the hot air stream and eff is the heat exchanger effectiveness, which is found using a lookup table based on the surface treatment, geometry, and material of the heat exchanger. The hot fluid properties, including temperature are determined by the inlet and outlet flow chambers. The fluid temperature is found using the energy equation as shown below.

$$\frac{dT}{dt} = \frac{Q_{heat\ transfer} + \dot{m}h_{in} - \dot{m}h_{out} - \frac{d(m_v)}{dt}U}{m_v C_{vf} + m_{wall} C_{vw}} \tag{27}$$

The cold pressure and the hot fluid mass flows are determined by look up tables based on the geometry and surface finish of the heat exchanger.

3.3.2. Component Exergy Derivation

By employing the 2nd law of thermodynamics, the efficiencies of the ACM and performance are captured. An exergy analysis provides insight into the available energy of the system and exactly where the inefficiencies of the machine are located. By

analyzing the exergy destruction rate, the quantity of the work capacity that a system loses during a process is quantified. To fully assess the total irreversibility in the ACM, a system level approach was taken. By modeling the individual components within the ACM model, the inefficiencies within the total ACM can be more directly analyzed. The main components studied include the turbine, compressor, and heat exchanger. These are the core system components of the ACM and are the main source of exergy destruction. The development of the exergy destruction model is described in the following sub sections.

Turbine/Compressor

The equations below are used to calculate the rate of exergy destruction for the turbine and compressor sub systems used in the ACM. Mathematically, these two have identical exergy destruction computations. Both are developed on a molar basis for a more robust model.

$$\dot{X}_{dest} = \dot{m}\frac{T_0 \Delta s_{gen}}{\bar{M}_{avg}} \tag{28}$$

$$\bar{M}_{avg} = x_{air} * \bar{M}_{element} \tag{29}$$

$$\Delta s_{gen} = c_P * ln\frac{T_{out}}{T_{in}} - R_u * ln\frac{P_{out}}{P_{in}} \tag{30}$$

The turbine and compressor exergy equations used in this work were developed and implemented in the model. Through this analysis, the total exergy destruction through the turbomachinery of the ACM was quantified.

Heat Exchanger

The heat exchanger exergy balance equations used in this work were developed and implemented in the model. The model splits the heat exchanger into three different flow streams to compute the transient entropy generated: 1) the cold side flow, 2) the hot side flow, and 3) the heat exchanger mass. The equations below are used to calculate the exergy balance of the heat exchanger, where c is for cold air, h is for hot air and HX is for heat exchanger. These assume constant mass in the control volume and constant pressure.

$$m_c \frac{c_{p,c}}{T_c}\frac{dT}{dt} = \frac{-\dot{Q}_c}{T_{HX}} + \dot{m}\left(s_{in,c} - s_{out,c}\right) + \dot{S}_{gen,c} \tag{31}$$

$$m_h \frac{c_{p,h}}{T_h}\frac{dT}{dt} = \frac{-\dot{Q}_h}{T_{HX}} + \dot{m}\left(s_{in,h} - s_{out,h}\right) + \dot{S}_{gen,h} \tag{32}$$

$$m_{HX} \frac{c_{p,HX}}{T_{HX}}\frac{dT}{dt} = \frac{\dot{Q}_c + \dot{Q}_h}{T_{HX}} + \dot{S}_{gen,HX} \tag{33}$$

By utilizing the additive property of exergy, the overall exergy destruction rate for the heat exchanger is found by,

$$\dot{X}_{dest} = -T_0(\dot{S}_{gen,cold} + \dot{S}_{gen,hot} + \dot{S}_{gen,HX}) \tag{34}$$

$$\dot{X}_{dest} = -T_0 \begin{pmatrix} m_c \frac{c_{p,c}}{T_c}\frac{dT}{dt} - \dot{m}\left(s_{in,c} - s_{out,c}\right) \\ + m_h \frac{c_{p,h}}{T_h}\frac{dT}{dt} - \dot{m}\left(s_{in,h} - s_{out,h}\right) \\ + m_{HX} \frac{c_{p,HX}}{T_{HX}}\frac{dT}{dt} \end{pmatrix} \tag{35}$$

This provides a fully transient model of the heat exchanger utilized within the ACM. With the above development of the exergy destruction rate model for the heat exchanger, the overall exergy destruction rate for the ACM during operation was assessed. Both transient and steady state values were studied in order to fully understand the behavior of the ACM.

4. RESULTS

The results shown are that as simulated by the ACM Simulink model. It is important to note that the results are not that of the experimental bench top test stand of the ACM. Although this work compliments that of the experimental work, the simulation results are separate. The model was developed based on the bench top test stand of an ACM developed and is used for accurate, predictive measures of the experimental ACM.

4.1. Preliminary ACM Analysis

The ACM model after full development is shown in Figure 7. As seen, the main inputs included are the house (compressed) air, fan cross flow, ambient air conditions, inlet pressure, and inlet heater load. By varying each of these boundary conditions, the ACM can be simulated in a number for different ways. Each input can be changed to emulate the different environments the ACM will operate in. The main controlling variable for the ACM is the inlet pressure as this is directly controlled by a regulating valve and will determine the performance of the ACM. The other inputs can be viewed as disturbances or environmental variables in that they vary with different simulations, but these cannot be directly controlled in a typical ACM setup.

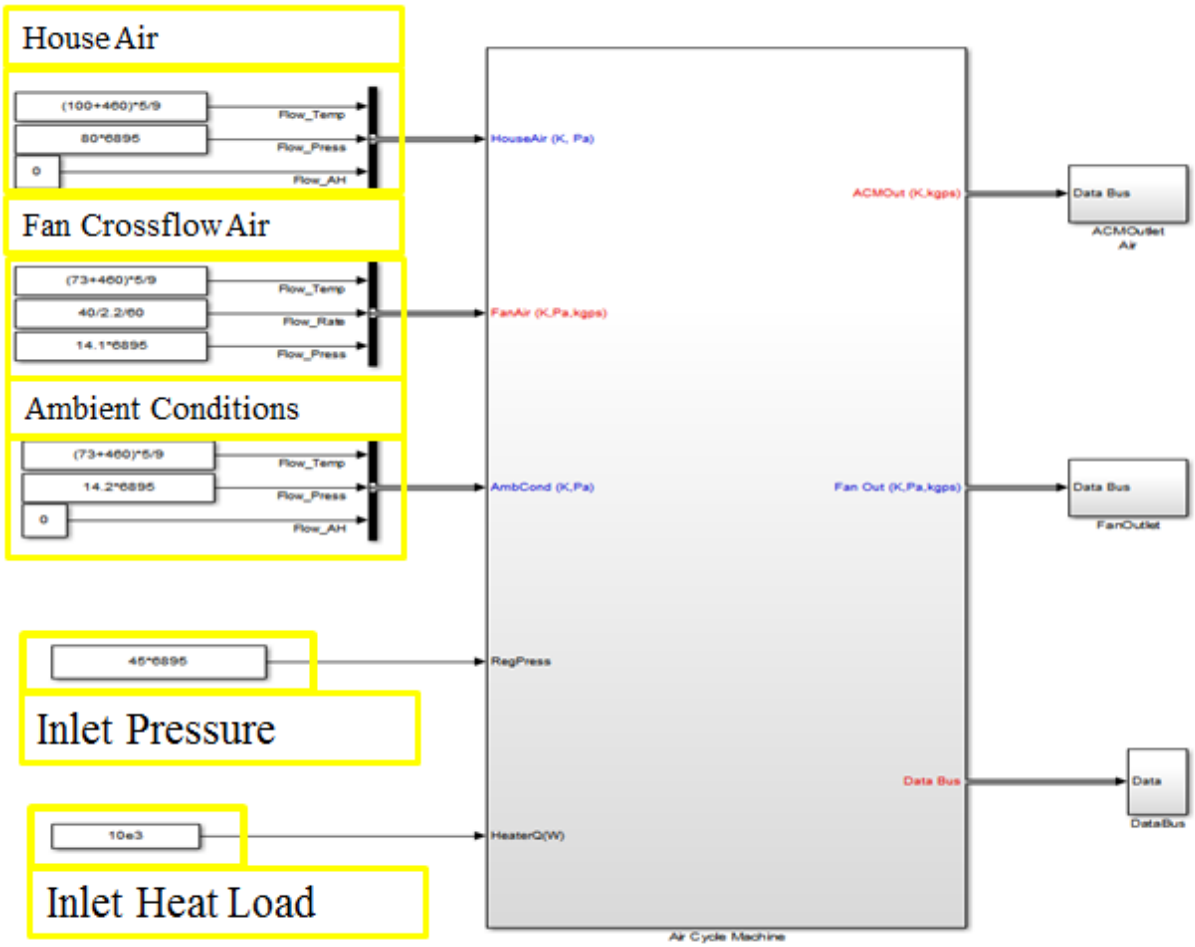

Figure 7. ACM Simulink model with boundary conditions.

For a baseline simulation, the ACM simulation run conditions are given in Table 1. The model takes the tabulated values as inputs and performs a transient study over a set period of time. The preliminary simulation was run for 200 seconds. These variables can be dynamically changed throughout the mission simulation to better emulate the varied operating characteristics of an ACM onboard an aircraft.

Table 1. ACM model parameters

Signal Name	***Value***	***Units***
Facility Air Temperature	80	F
Facility Air Pressure	100	psia
Facility Air Absolute Humidity	0	lbm/lbm
Fan Air Temperature	73	F
Fan Air Pressure	14.1	psia
Fan Air Mass Flow	60	ppm
Ambient Conditions Temperature	73	F
Ambient Conditions Pressure	14.2	psia
Absolute Humidity	0	lbm/lbm
Regulator Pressure	30	psia
Heater Q	20	kW

For this simulation, the ACM did not have a specified cooling load constraint that it must meet. This allowed the simulation to be run without a controller providing flexibility in studying the response of the ACM to the critical input parameters. The simulation results are the temperature, pressure and mass flow at each of the defined state points of the ACM. The simulation also captures the turbomachinery shaft speed of the ACM. The states are the compressed air within the reservoir (point 0), the air after passing through the resistive heater (point 1), air after passed through the regulating valve (point 2), air after the compressor (point 3), air after the heat exchanger (point 4), and the air after turbine (point 5). The air after the cooling turbine at point 5 is used as the coolant to the

load defined for the ACM. This load is representative of various load demands a typical ACM can handle such as cockpit environment cooling or avionics cooling. Figure 8 presents the temperature simulated for the ACM station points.

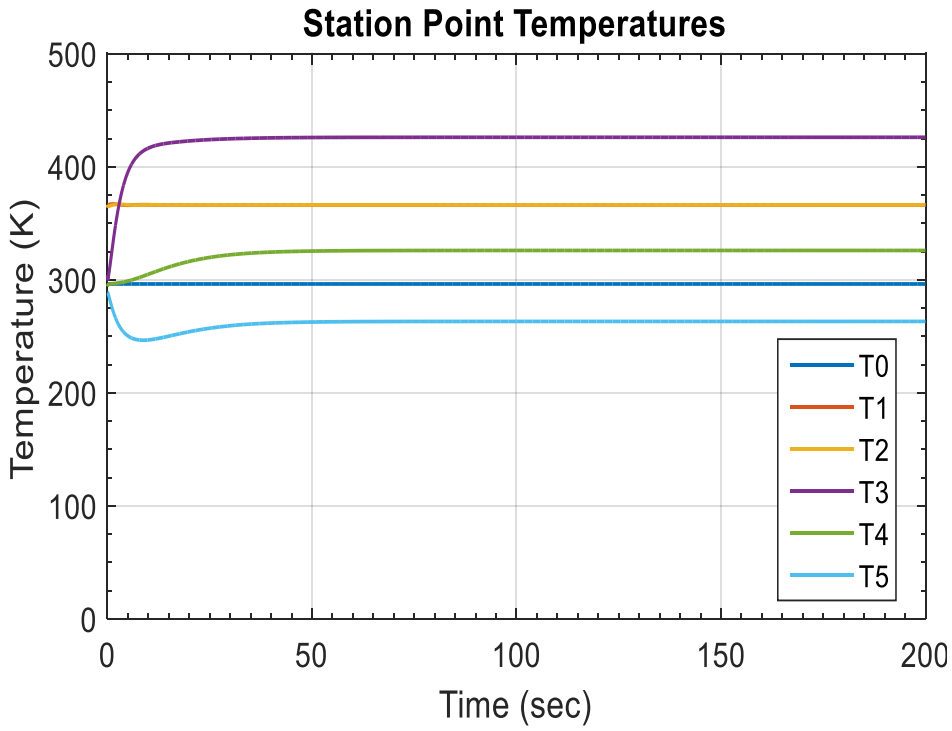

Figure 8. State point temperature for the ACM.

The temperature, T_5, at the exit of the cooling turbine is colder than the initial temperature. This sanity check demonstrates that the ACM is operating as a cooling mechanism. The temperatures at each state are as expected: a rise in temperature after the heater, temperature rise after compression, a drop in temperature across the heat exchanger and the final temperature drop after the turbine. The transient period for the ACM should also be noted. Before the operating temperatures of the ACM reach steady state conditions, there are significant dynamics of the ACM that are captured.

Shown in Figure 9 are the state point pressures for the ACM throughout the simulation. The results follow the expected trend. The pressure drop due to the flow across the heat exchanger, P_3 to P_4, can also be seen but is not large compared to the drop across the turbine.

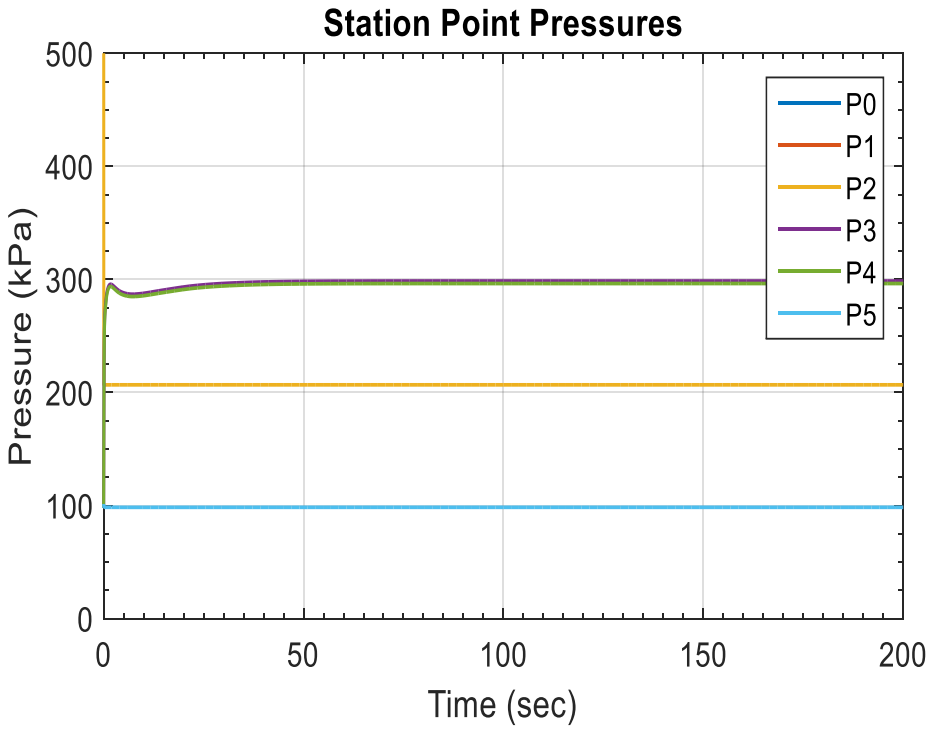

Figure 9. State point pressures for the ACM.

The system mass flow through each state point is shown in Figure 10. Here it is important that the mass flow through each component is constant throughout the system simulation to ensure the law of mass continuity is followed. There is a transient startup period where the mass flow throughout the system dynamically changes before the steady state value is reached.

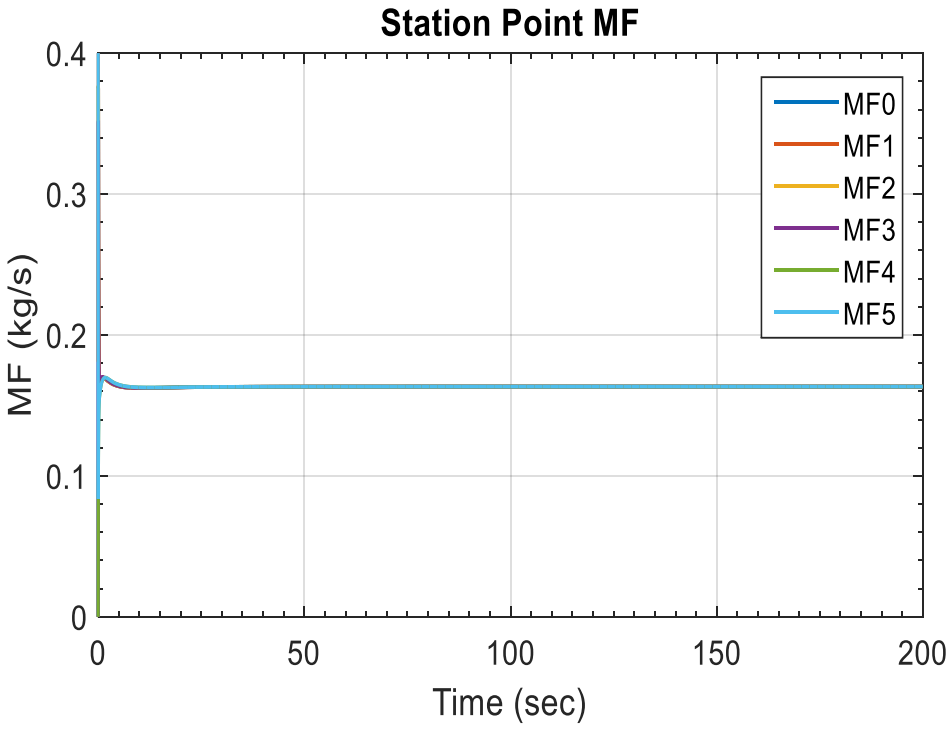

Figure 10. State point mass flows for the ACM.

The turbomachinery speed (shaft rotational speed) is also simulated and shown in Figure 11. The shaft speed is as expected for this type of simulation.

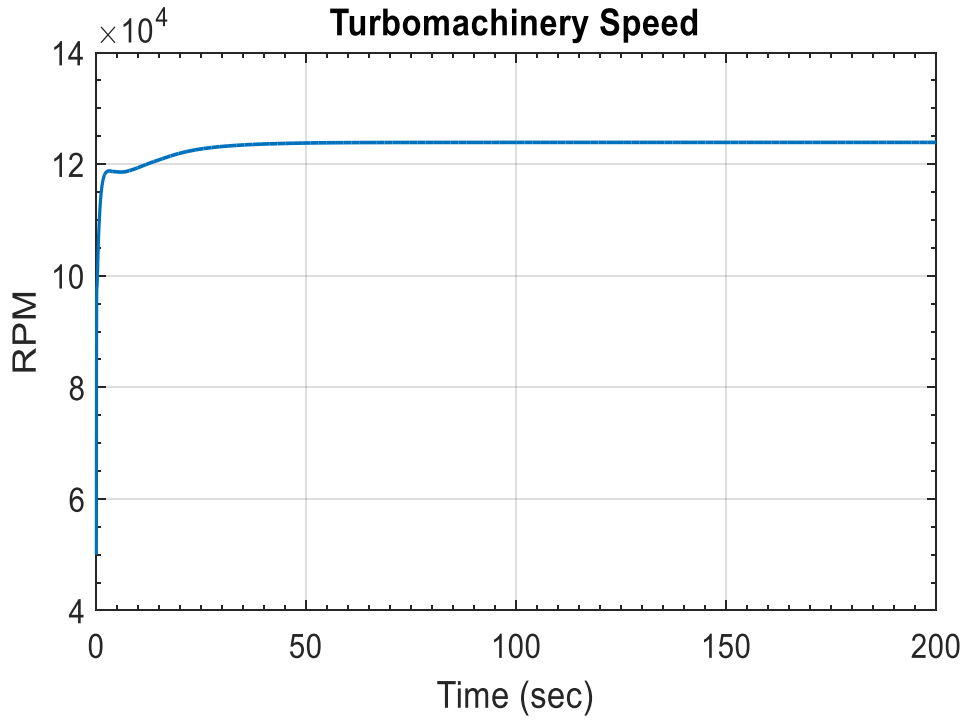

Figure 11. ACM shaft speed for turbomachinery.

While the results shown above quantify the behavior of the ACM, the performance is not characterized and no information is given to optimize the performance. In order to do this, the exergy destruction rate for each of the core components of the ACM must be quantified.

4.1.1. Exergy Analysis

Shown in Figure 12 are the exergy destruction rates for the core components of the ACM, the turbine, compressor, and heat exchanger. The transient response of the heat exchanger is much larger than that of the turbomachinery. This is due to the nature of thermal progression across the heat exchanger. The important information shown here is that the heat exchanger has significantly larger exergy destruction through its startup period than the turbomachinery. The finite temperature difference across the heat exchanger is the

reason for this behavior. Because the heat exchanger is oversized for the specific turbomachinery used, the exergy destruction rate is much larger than the turbomachinery. This heat exchanger was chosen to achieve the maximum temperature drop between the compressor and turbine. Over time, the steady state values for each of the components level off to roughly the same value and behave normally. Therefore, when looking at optimization and transient controls of the ACM, the heat exchanger is the driving component that must be studied.

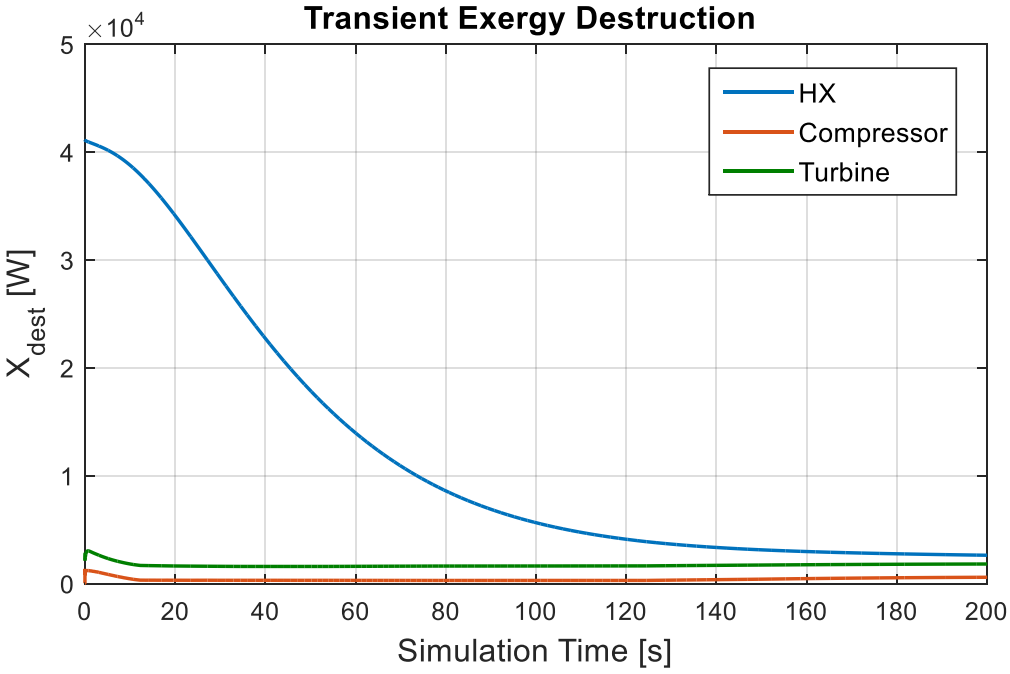

Figure 12. Transient exergy destruction rate for ACM components.

Shown in Figure 13 is the combined exergy destruction rate for the ACM. This is the combination of the compressor, turbine, and heat exchanger exergy destruction rate throughout the transient period of the ACM simulation. As previously determined, the heat exchanger is the main component that drives the exergy destruction during the transient operation.

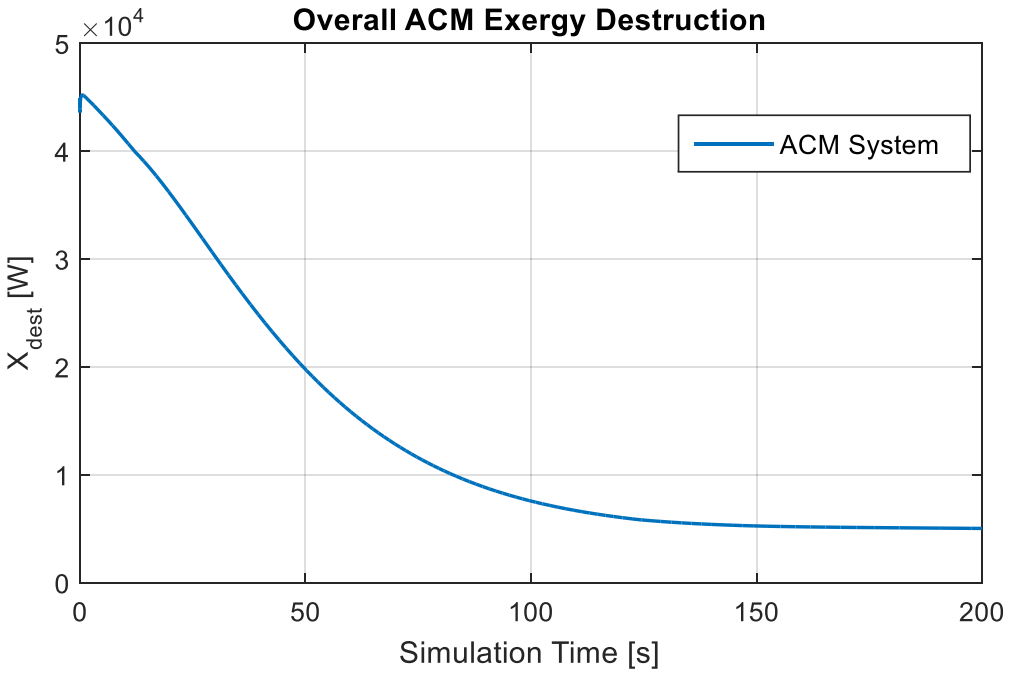

Figure 13. ACM transient exergy destruction rate.

To further investigate the transient behavior of the exergy destruction rate for each of the core components of the ACM, another simulation with a disturbance in the inlet heat load for the resistive heater was run. The simulation time was also increased to better investigate the full behavior of the ACM. The disturbance was setup such that at simulation time, t = 1000 s, the input power of the heater was raised from 10 to 15 kW. This emulates a sudden rise in temperature for the incoming air to the ACM onboard an aircraft which could be seen during flight operation in a mission profile. Figure 14 displays how each component responds to this sudden increase of inlet air to the ACM.

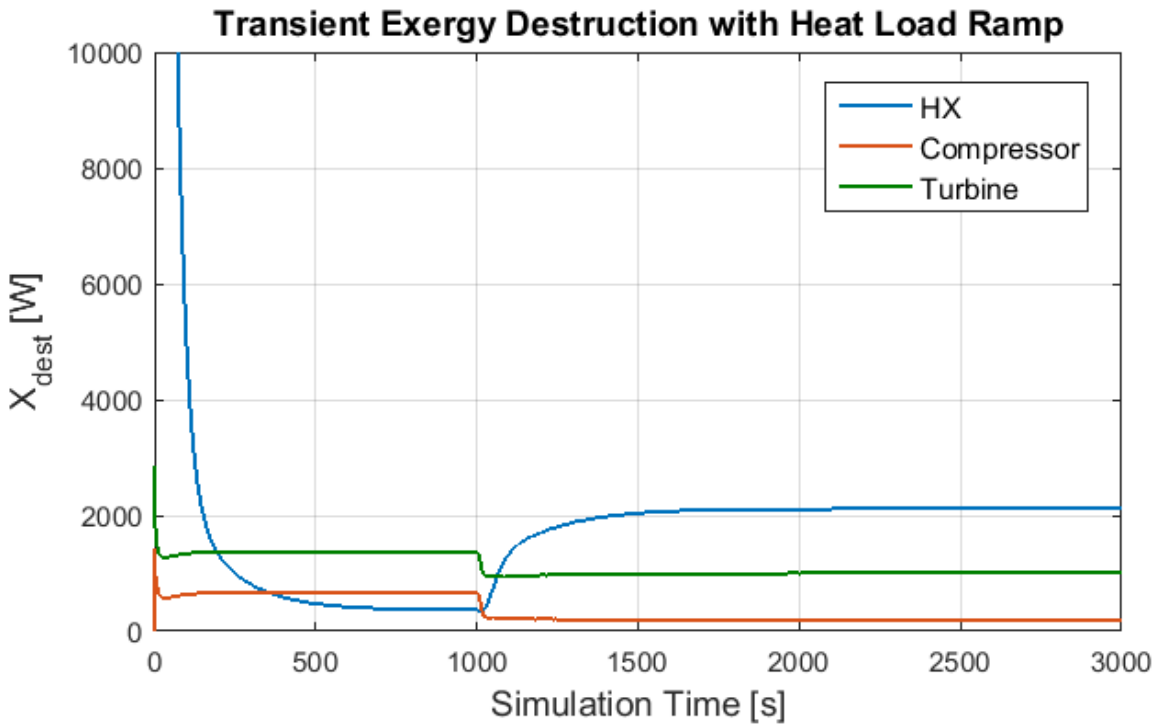

Figure 14. ACM component exergy destruction rate with sudden increase in inlet air temp.

Because the air for an ACM is from bleed air off the engine, when an aircraft has a sudden rise in power demand for the engine, the ACM will have to dynamically adjust to the increased load of the incoming air. Again, the heat exchanger is the main component that will drive the transient operation of the ACM. Interestingly, the turbine and compressor both see a decrease in exergy destruction with the increase of inlet air. This is because the turbomachinery was designed for high temperature environments and operates at higher efficiency with the increase in temperature at the inlet of the compressor. These initial results for the ACM model point to the ACM's potential to be optimized during the transient operation.

4.2. ACM Operation with Cooling Constraint

A cooling constraint was then added to the ACM. The cooling load that the ACM needs to meet is modeled as a heat load rate at a given environment temperature. This load represents the demand the ACM is needed for such as cooling the cockpit or the avionics onboard. By adding this constraint, the ACM model more accurately represents how an ACM onboard an aircraft is implemented. For this investigation, the cooling demand is an input that can be varied depending on the mission desired. The ACM's inlet pressure is then controlled with a PI controller to meet this constraint added to this system. Controlling the inlet pressure is the common method used to control the ACM performance as the typical ACM operates off of the bleed air from the engine.

4.2.1. System Response

In the control framework for the ACM, there are two primary objectives. The first is to meet a specified performance demand given as a cooling load. The cooling load should be reached in a reasonable time so as not to hinder the operation of the total thermal management system. This acts as a primary performance constraint on the system. The second is to maximize system efficiency through EDM and optimal control. The optimal control is captured by implementing smart controls of the ACM that take into account the different operating environment of the ACM and transient behavior throughout the simulation.

Studying the ACM response, the system exhibits either an overdamped or underdamped response depending on the controller gains. For the underdamped case, the system response oscillates before reaching the steady state value. This overshoot can cause inefficiency in the transient operation of the system. Exergy destruction is used as the

measurable variable to determine exactly how much inefficiency is introduced from the percent overshoot. It is desirable to obtain the optimal controls such that there is not a large percent overshoot. However, the underdamped system has a much quicker response time than that of the overdamped system. This tradeoff between speed to reach the cooling demand and operational efficiency is the struggle that the control design must tackle. Shown in Figure 15 is the ACM system response to the cooling demand set in the simulation when the system is underdamped.

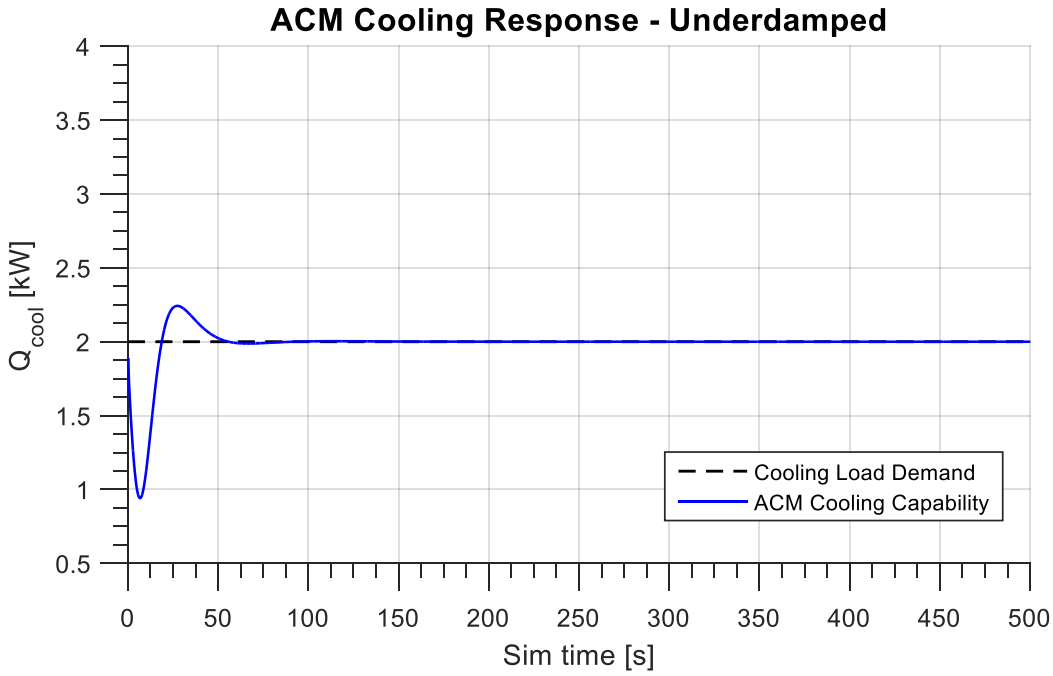

Figure 15. ACM response when underdamped

For the underdamped system, the exergy response exhibits a significant spike in the exergy destruction in the early transient period of operation. This spike is due to the overshoot caused by the underdamped control system. By implementing the EDM approach, this spike should be eliminated. This is done by employing different system controls with an overdamped controller.

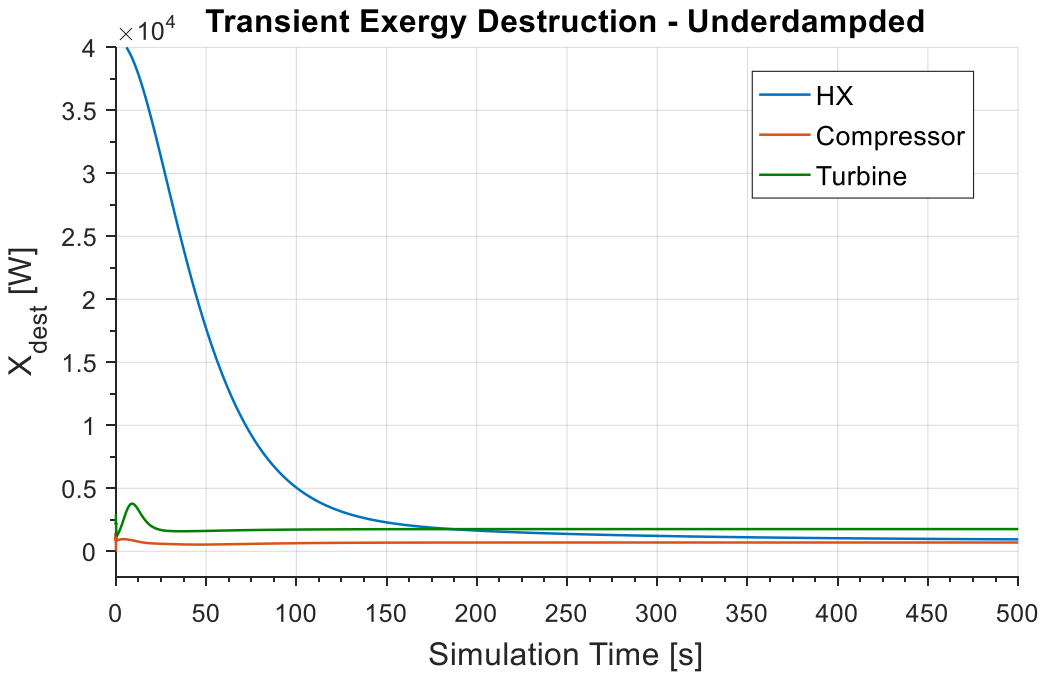

Figure 16. Transient exergy destruction rate for underdamped ACM controls.

The counterpart to the underdamped system is setting the controller gains in such a way that the system is overdamped. When the system is overdamped, the response time is considerably larger than when underdamped. This increase in response time can prove to critically affect the performance of the TMS aboard the aircraft. However, the exergy destruction rate for the overdamped case is lower than that for the underdamped system. Shown in Figure 17 is the overdamped ACM system response for a constant cooling load.

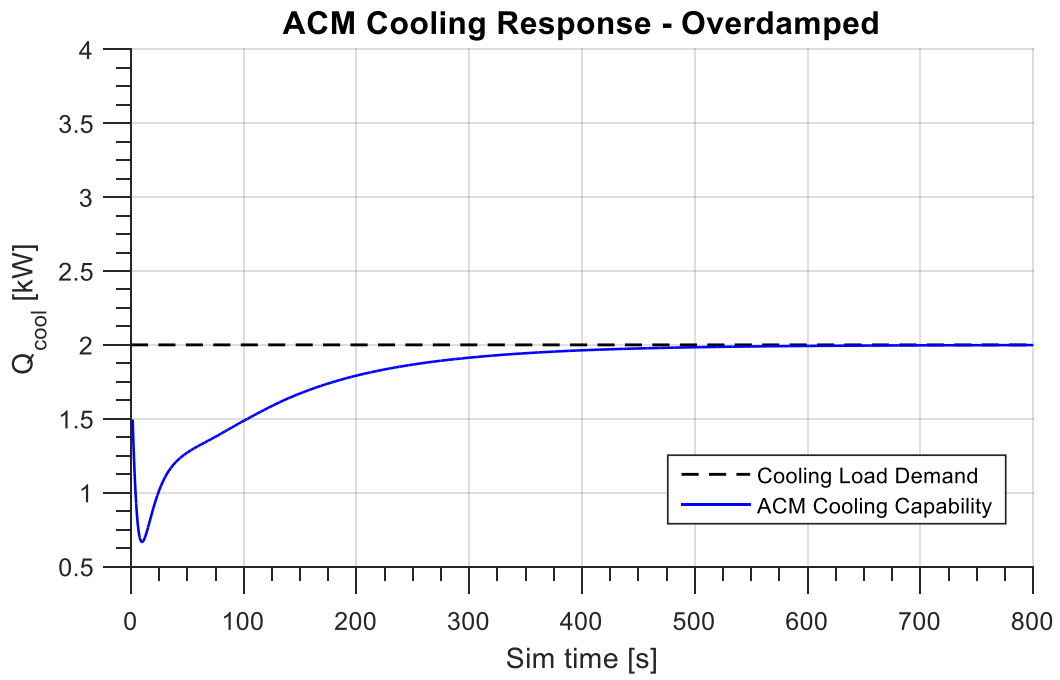

Figure 17. ACM response when overdamped

The response time to reach steady state is an order of magnitude larger than that of the underdamped system. The overdamped system takes approximately 500 seconds to reach steady state whereas the underdamped only takes around 50 seconds. For the overdamped system, the transient exergy destruction rate for the ACM is less than that of the underdamped system. Figure 18 displays the values of the exergy destruction rate for the ACM when overdamped.

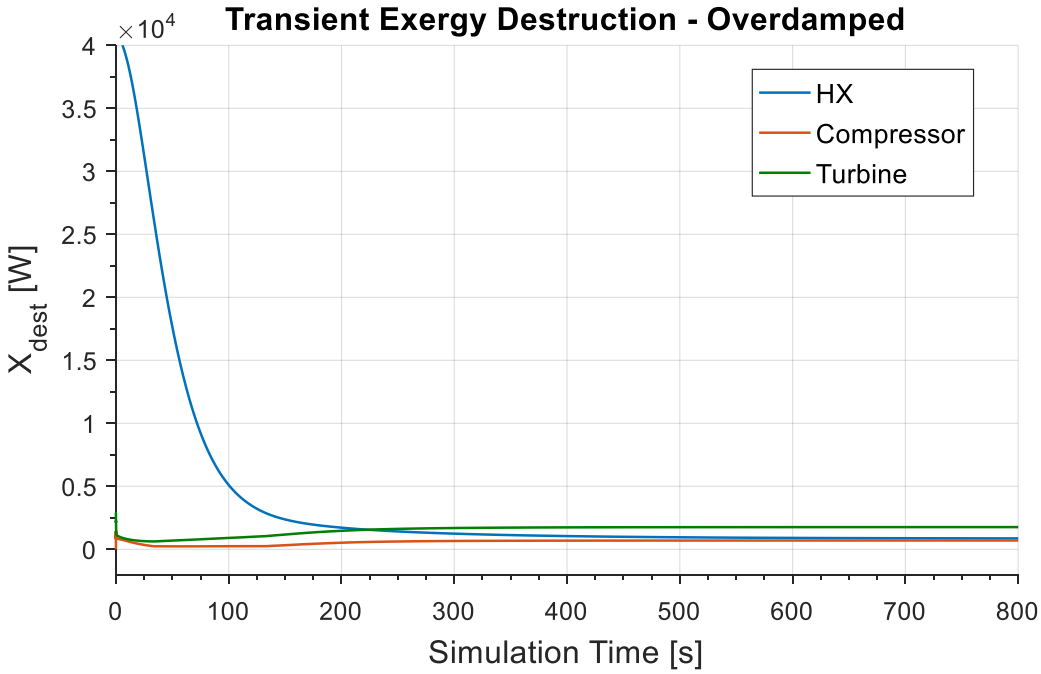

Figure 18. Transient exergy destruction rate for overdamped ACM controls.

The exergy destruction rate does not experience a spike and has a lower overall exergy destruction value for the entirety of the simulation. This results in higher system efficiency throughout the simulation. This, however, does come at a cost. As seen with the system response, the cooling capability of the ACM takes longer to reach the cooling demand of the aircraft.

To better quantify the system response to both overdamped and underdamped controls, simulations were coordinated where the system controller was designed with specific damping ratios, zeta. Four controllers were designed each with differing damping ratios. By changing the cooling demand from 2kW to 3kW at time = 2000 seconds within the simulation, the transient exergy destruction rate was studied as a function of damping ratio. While this is only a single step change for the cooling demand, a typical ACM will have multiple changes in the cooling demand throughout an entire mission. Therefore, it

is important that for each change, the transient response of the system does not have high inefficiencies associated with the operation.

Figure 19 displays the exergy destruction rate for the ACM with zeta values of 0.35, 0.60, 0.707, and 1.25. For the overdamped systems, zeta of 0.35 and 0.60, the system exergy destruction rate response has a large spike in exergy destruction when the cooling demand step takes place at time = 2000 seconds. This transient behavior of exergy destruction rate should be minimized in order to optimally control the ACM system as it operates in real time. For the overdamped system, zeta of 1.25, there is not a spike in the exergy destruction rate. However, the system response is significantly slower than desirable. For the case where zeta is set to a critical value of 0.707, the system behaves as desired. The response time is reasonable without a large spike in exergy destruction rate causing high inefficiencies in the system operations during transient periods. For each of the cases, the heat exchanger did not have a large change in exergy destruction rate as observed in Figure 16 and Figure 18. This is due to the fact that the exergy destruction rate at the initial startup of the ACM for the heat exchanger will be uncharacteristically higher due to the large delta in temperatures for the cross flowing air streams. Once the air flow temperatures across the heat exchanger reach a steady state operating point, the exergy destruction will remain relatively constant even for increased cooling demand. There is a small increase in the exergy destroyed for the heat exchanger with an increase in cooling demand, but the turbine and compressor have a larger increase that will cause higher inefficiencies in the ACM system operation.

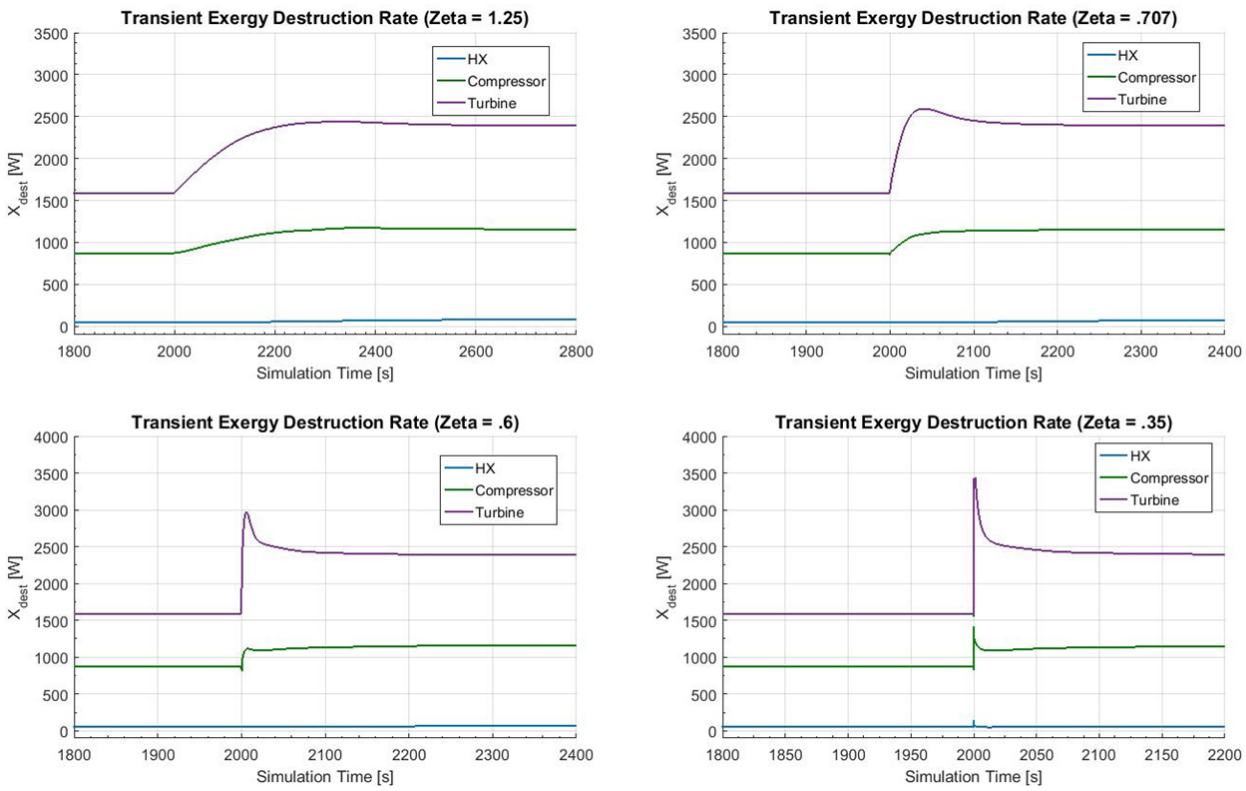

Figure 19. Transient exergy destruction rate for varying damping ratios, zeta

To further investigate the total effect the damping ratio has on performance, the total exergy destroyed throughout the simulation was tabulated for each control design. Table 2 presents the overall exergy destroyed for each of the core ACM components for the varying damping ratios. The turbine had the largest effect on the exergy destruction for the ACM simulation and represents the largest contribution to the exergy destruction spike during transient operations.

Table 2. Exergy destroyed during simulation with cooling demand step change

	Exergy Destroyed (kJ)			
ACM Component	**Zeta = 1.25**	**Zeta = 0.707**	**Zeta = 0.60**	**Zeta = 0.35**
Turbine	5451	5537	5628	5712
Compressor	2751	2798	2866	2909
Heat Exchanger	2560	2564	2566	2601
ACM Exergy Destroyed	**10762**	**10899**	**11060**	**11222**

It is desirable to obtain controls such that the system reaches the cooling potential quickly but also in an efficient manner. This correlates to minimizing the overshoot caused by a quick system response but ensuring the response is fast enough to meet the cooling demand in a reasonable time. These two constraints oppose each other driving the need for an optimal balance. As the response time decreases allowing the ACM to meet the cooling demand faster, the exergy destruction rate for the ACM tends to have a spike during transient operation. This spike is wasted potential work of the ACM that is lost. The counter part of this is relaxing the time constraint on the cooling response of the ACM system. Increasing the response time for the ACM cooling will actually decrease the exergy destruction rate during transient operation. This decrease in exergy destruction rate associates to a higher operating efficiency because less work is lost to irreversibilities. Accounting for these constraints is not the only consideration for the design of optimal controls for the ACM. In addition, the controls must also be able to take into account the environmental changes for the ACM's boundary conditions throughout a mission.

4.3. System Optimization

To emulate the varied mission profile the ACM may encounter, a simulation is set up such that during operation there are disturbances in the boundary conditions as well as changes in the cooling demand. The dynamic boundary conditions include the heat load applied to the inlet air of the ACM and a change in the accessible ram air for the heat exchanger. These two parameters both vary throughout a mission and can drive the ACM to operate with high inefficiencies. The cooling demand is also changed to demonstrate how the ACM can react to an increase in demand by the aircraft. To compensate for these changes, the controls used for the ACM must be designed to dynamically update based on the input parameters and cooling demand. Table 3 presents the parameters for the ACM simulation that are of interest. Shown are the ranges of the signals that each variable has been set to simulate. These ranges are limited by the constraints of the physical, bench top testing unit and how the experimental ACM unit was designed. The operator can simulate different environments based on these signals into the ACM model.

Table 3. ACM mission simulation parameters

	Model Signal	Range of Values
Boudnary Conditions	Inlet Heat Load (Inlet Temp)	5 - 20 kW
	Ram HX Crossflow	0 - 0.45 kg/s
	Ambient Air	20 C ; 101 kPa
Constraints	Cooling Demand	1 - 4 kW
	Exergy Destruction	Minimize
	Response Time	Optimize
Control Variables	Inlet Pressure (Inlet Mass Flow)	172 - 345 kPa
	Control Gains	Mission Specific

For the system simulation, an inlet heat load of 10 kW was used. The available ram air for the heat exchanger was set to a value of 0.45 kg/s. The dynamic change throughout the mission simulation is an increase in the cooling demand. The cooling is increased from a 2 kW load to 4 kW at t = 2000 s. During the ACM operations, each of these conditions can and will continuously change throughout a mission profile. To compare multiple controller designs, four sets of controller gains were used for the described simulation utilizing the boundary conditions tabulated above. Figure 20 shows the response of the ACM cooling system for four different control designs each varying in how the system is controlled.

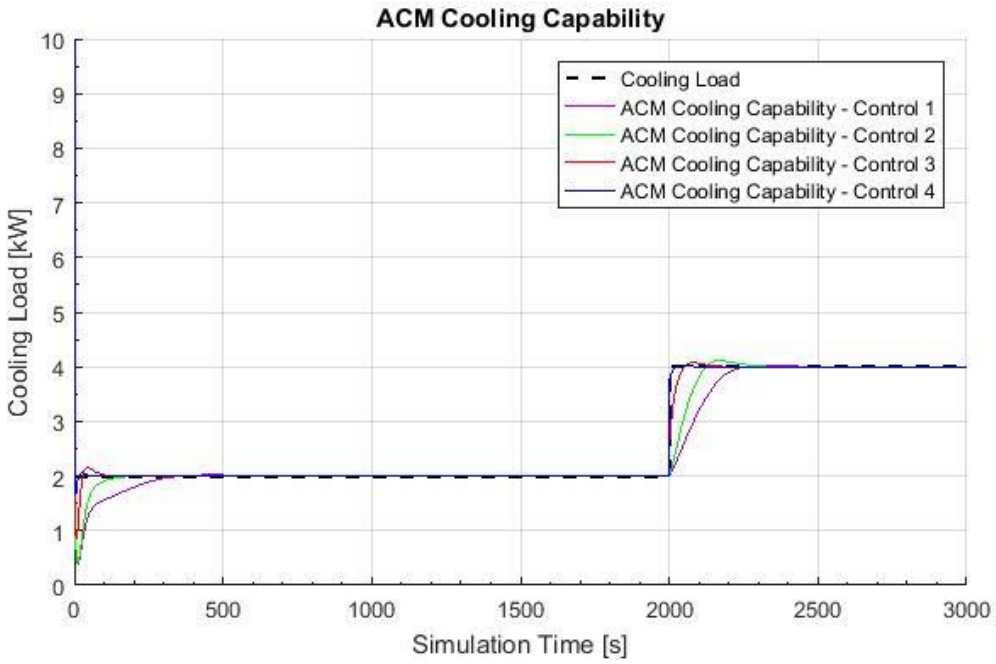

Figure 20. ACM cooling response to increased cooling demand.

As seen above, the ACM system response is largely determined by the controller design. The optimized controller design for the above simulation is Control 4. While this controller is suitable for the given boundary conditions of inlet heat load and available ram air, this controller will behave differently as these parameters are dynamically changed throughout the simulation.

The change in controller behavior is explored by comparing the controller design at two different boundary conditions. The boundary conditions were changed from BC #1 where the inlet heat load was 10kW and the available ram air for the heat exchanger was 0.45 kg/s to BC #2 where the inlet heat load was 15kW and the available ram air was 0.3 kg/s. Figure 21 displays the comparison between the two different responses of the ACM when the controller design is the same for varied boundary conditions.

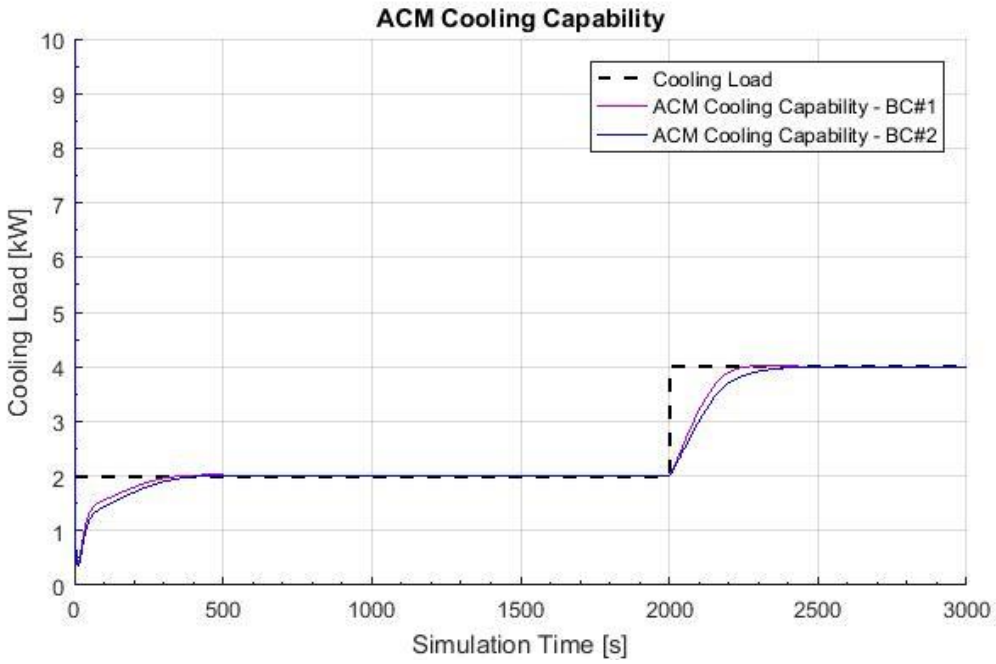

Figure 21. ACM cooling response for varied boundary conditions.

While the difference may be seemingly small, any change in the boundary conditions can cause a more dramatic variation in how the ACM is controlled and therefore degrading the performance. This drives the need to look at the ACM system over a known operating band for a set of boundary conditions and develop smart controls for each potential boundary condition the ACM may experience.

4.4. Control Design

Because the ACM experiences varied boundary conditions throughout its operation, such as perturbations at the inlet temperature and varying ram airflows, the control design must compensate for the fluctuations in the boundary conditions. Gain scheduling is a common strategy for controlling systems, such as the ACM, whose dynamics change with such variables. A gain-scheduled controller is a controller whose gains are automatically adjusted as a function of time, operating condition, or plant parameters and

seeks to optimize the system process for a given set of operational points [37]. A scheduling mechanism to update the PI gains of the system controller was implemented based on the inlet temperature to the ACM and the ram crossflow across the heat exchanger. Here, optimal performance is defined as a balance between minimizing the response time to reach the cooling demand without creating large system inefficiencies measured by the exergy destruction rate. In practice, designing a set of controllers specific to varying parameters for the ACM, inlet heat load and ram air crossflow, requires a series of specific steps commonly taken in control design.

The ACM model must be transformed into a state space model given by a system of linear equations. The dynamics of the systems are expressed as differential equations in the general form as the following.

$$\partial x(t) = \bar{\mathrm{A}}\,\partial \mathrm{x(t)} + \bar{\mathrm{B}}\,\partial\,\mathrm{u(t)} \tag{36}$$

$$y(t) = \bar{\mathrm{C}}\,\partial \mathrm{x(t)} + \bar{\mathrm{D}}\,\partial \mathrm{u(t)} \tag{37}$$

The coefficients $\bar{\mathrm{A}}, \bar{\mathrm{B}}, \bar{\mathrm{C}}, \text{and } \bar{\mathrm{D}}$ of the states are known as the Jacobian matrices of the system. In order to create the linearized state space model for the ACM, first the plant model must be trimmed at all the operating points, or boundary conditions, of interest. In theory, this is done by solving for x(t) at the equilibrium operating point , X_0. Once the model is trimmed for a given set of boundary conditions, a batch linearization must be completed for each of the varying boundary condition variations, inlet heat load and ram air crossflow. For the ACM, the boundary conditions were limited to a discreet number of points in the range of 5-20 kW for the inlet heat load and 0 – 0.45 kg/s for the ram air

crossflow. Given below are the Jacobian matrices for the state space model for the ACM model. The ACM has a total of 17 states describing the dynamics of the plant model each of which are include within the state space model. Each of the 17 states are specified nodes at the inlet/outlet of systems within the ACM such as the heater, turbine, heat exchanger, etc.

$$\overline{\mathrm{A}} = \begin{bmatrix} a_{1,1} & a_{1,n-1} & a_{1,17} \\ a_{n-1,1} & a_{\ldots} & a_{\ldots} \\ a_{17,1} & a_{\ldots} & a_{17,17} \end{bmatrix} \tag{38}$$

$$\overline{\mathrm{B}} = \begin{bmatrix} b_1 \\ b_{\ldots} \\ b_{17} \end{bmatrix} \tag{39}$$

$$\overline{\mathrm{C}} = \begin{bmatrix} c_1 & c_{\ldots} & c_{17} \end{bmatrix} \tag{40}$$

$$\overline{\mathrm{D}} = [d] \tag{41}$$

By creating the Jacobian matrix for N-number of boundary conditions specified within the range for inlet heat load and ram air crossflow, a 2D grid of linearized plant models for the ACM that describe the model dynamics is built. Once each of these systems is characterized, a family of linear controllers for the plant models must be designed for each state space system by using the optimization criteria of minimizing response time and overshoot without a substantial increase in exergy destruction. Finally, a scheduling mechanism is designed such that the PI controller gains change based on the values of the scheduling variables/ boundary conditions of the plant models.

This technique allows for the model dynamics to be analyzed and better quantify the effects of the transient response for varying controller gains. The ACM controller will

dynamically update its gains to reach a desired damping ratio of 0.707 based on the varied inlet temperature conditions and the varied available ram air for the heat exchanger. Another approach that was not used would be to build a parametric gain surface for the system controller. A parametric gain surface is a basis-function expansion whose coefficients are tunable to meet the scheduling demand. The parametric gain surface creates smooth transitions between system operating points. In future work, this approach may prove beneficial to creating a smarter, more sophisticated controller.

Once the scheduling mechanism was implemented into the model, a final simulation was set up to analyze the behavior of the ACM control architecture for varying boundary conditions and performance criteria. Shown in Table 4 are the parameters varied throughout the simulation along with the timestamp each change occurred.

Table 4. ACM Simulation Parameters

Parameter	***Initial Value***	***Final Value***	***Time of Change***
Ram Air Crossflow	.38 kg/s	.45 kg/s	t = 1000 s
Inlet Heat Load	10	20	t = 500 s
Cooling Demand	2	3	t = 2000 s

Shown in Figure 22 are the step changes simulated in the ACM model's boundary conditions as tabulated in Table 4.

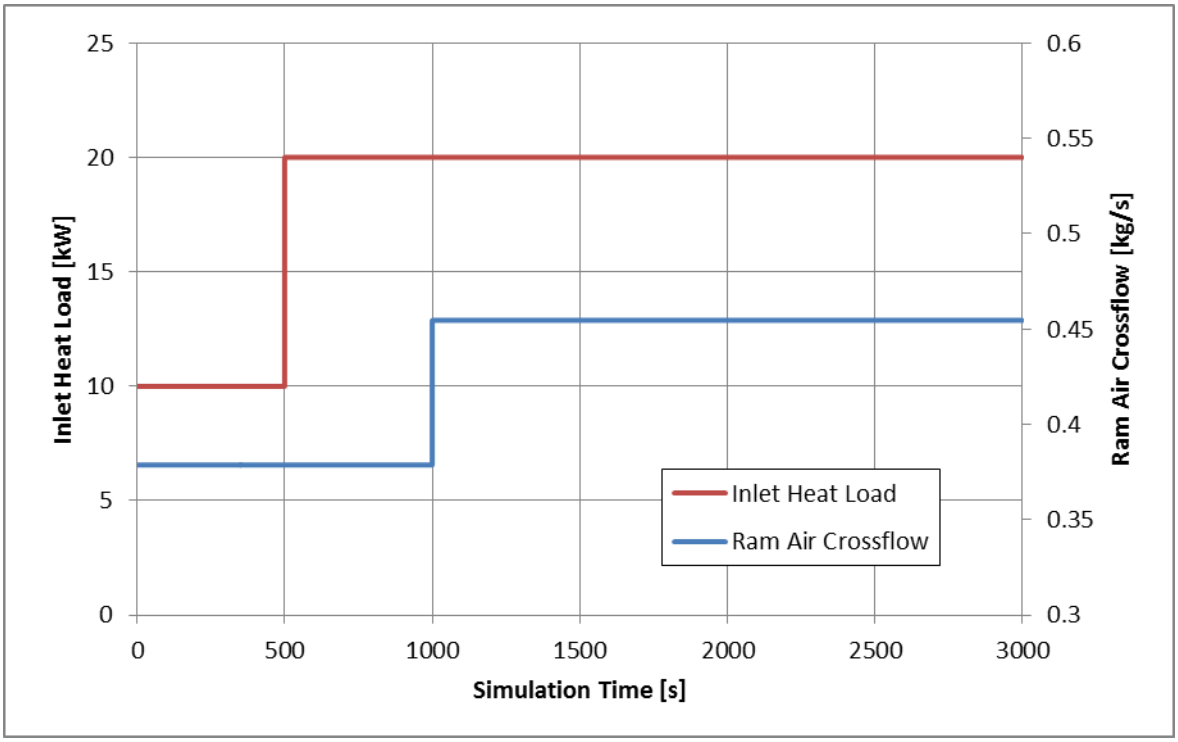

Figure 22. Boundary conditions for ACM during simulation

The total system exergy destruction rate is displayed in Figure 23. Shown here the ACM system exergy destruction rate is minimized without having large spikes during the mission even when the boundary conditions were changed. This has been achieved by appropriately designing the controls of the ACM to account for the varied load and boundary conditions.

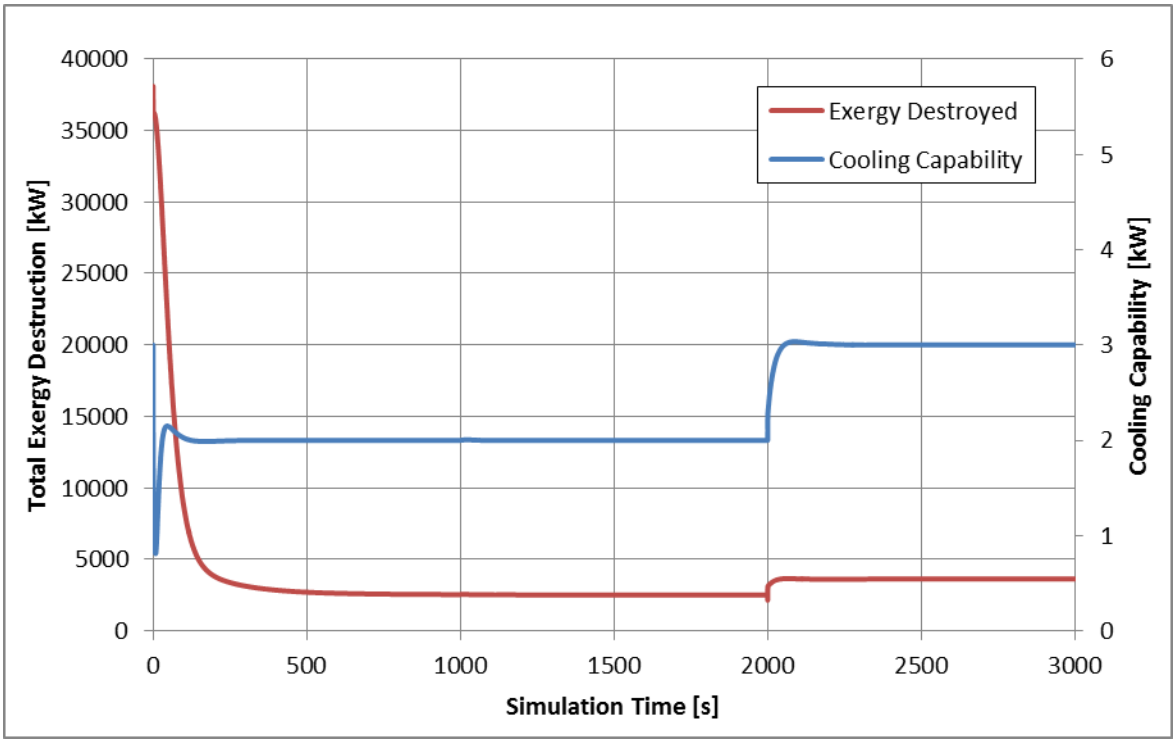

Figure 23. ACM total exergy destruction rate and cooling capability.

The exergy destruction rate however does have a large spike during the initial phase of the mission during transient startup. As mentioned earlier, this is due to the large time constant the heat exchanger has to reach steady state operating conditions. The increase at t = 2000s is due to the increase in cooling demand for the ACM. Again, there is not a spike during this period therefore the exergy destruction rate has been minimized accordingly.

5. SUMMARY OF FINDINGS

Through the use of modeling and simulation techniques, a full analysis was performed on a typical ACM setup found aboard aircraft. The entire model was developed within the MATLAB-Simulink ^{TM} environment. The analysis incorporated both a 1st and 2nd law

approach to quantify the overall performance of the system. The methodology used within this work can be utilized for future system models for various platforms. Final results through this analysis include:

- Each state point was modeled through the ACM cycle to include temperatures, pressures, mass flows, and turbomachinery speed.
- The model was created to emulate varied boundary conditions that are typically experienced throughout an aircraft's mission.
- An experimental test stand was designed for future use to validate the model.
- Through the use of a second law analysis which takes into account the exergy destruction, the system has a univariate performance factor that can be used across multiple system platforms and components.
- A dynamic control scheme was developed such that the ACM could meet a specified cooling demand. The optimal control design was discovered by associating the damping ratio to the system response time and exergy destruction.
- The total ACM rate of exergy destruction was characterized allowing for a systems level approach to optimization and system integration.
- Through transient analysis, the ideal range for control response was characterized based on exergy destruction and response time.
- A scheduling mechanism was implemented to allow the ACM to dynamically be controlled for the various environmental conditions it may experience throughout a flight mission.

6. CONCLUSION

To address the current and future thermal demands of aircraft, modeling and simulation techniques have been used to accurately predict behavior using physics based models of aircraft thermal management systems. One component that is incorporated in a typical TMS used within the environmental control system (ECS) is an air cycle machine. The ACM process follows the reverse Brayton cycle or Brayton refrigeration cycle where air is ultimately cooled through use of different thermodynamic components. This work focused on the development of an accurate model within the Simulink computational platform that is then used to optimize the control of the ACM. The modeling approach discussed combined both energy and exergy principles based on the 1^{st} and 2^{nd} law of thermodynamics. In contrast, only utilizing the traditional 1^{st} law analysis can leave out important information about the system operation that can lead to an inefficient design. Combining both these laws provided critical information about the system performance and outlines where system inefficiencies are. The optimization techniques used is based on an exergy based analysis. The specific approach utilizes the methodology of exergy destruction minimization where exergy destruction is looked at as a cost function for system operation. Along with control optimization, exergy destruction is also used for future integration of the ACM into larger, more complex system models. Due to the univariate nature of exergy destruction, it can be used across varied energy domains and is independent of the platform. This allows for multiple components, subsystems, and processes to be analyzed through a single performance characteristic. The exergy based approach used for the ACM is extensible to a systems-level assessment of more complex models.

The outputs of the dynamic model of the ACM include state point temperatures, pressures, and mass flows as well as turbomachinery shaft speed. Along with the state points, the exergy destruction was found for the core components of the ACM: the compressor, heat exchanger, and turbine. Once the overall ACM performance was captured within the model, a control schema was designed to account for the varied mission profile the ACM system may encounter onboard an aircraft. Varied boundary conditions such as inlet temperature, available ram air flow, and cooling demand were dynamically built into the model to emulate the ACM operation. To account for the varying parameters, a scheduling mechanism was designed for optimal control of the ACM at each boundary condition. This approach of gain scheduling can accommodate the multiple variants of operating conditions the ACM experiences throughout a mission and allows the systems to be fully optimized at each operating point. Through a rigorous exergy analysis of the ACM system, the method to optimize the system was defined by minimizing overshoot in the control of the inlet pressure without having a substantial lag in response time. While this outcome was expected, the approach can be applied to multiple systems the ACM works in tandem within the Thermal Management System. By combining the exergy analysis across multiple sub systems, a total efficiency parameter is defined allowing the complete system to be better studied and analyzed.

6.1. Future Work

For the advancement of this work, there are research paths that are recommended to further investigate the ACM and other TMS systems. First, the use of validation techniques should be done in tandem with the ACM model. This would include the use of the experimental test stand for further validating the results obtained from the ACM

model. A study could be performed to validate the exergy based analysis used within this work. Second, as the ACM system model becomes more complex, it is advisable to use more advanced computational techniques within the Simulink model so as not to slow the process simulation. As of now, the process is simulated relatively quickly but can be slowed greatly by addition of fidelity or other TMS systems. Therefore, to compensate for this additional demand, a rigorous study should be done as to pinpoint how to decrease the computational demand of the ACM simulation. Third, the ACM should be integrated into larger scale simulations. This would include other systems used within a TMS aboard and aircraft. The next logical step would be adding a vapor cycle system (VCS). This is because the two systems have interdependencies within a typical TMS architecture. By integrating the ACM with a VCS, the exergy based analysis can provide insight into how the two thermal systems interact and where system inefficiencies lie. Last, future work should study the methodology of controller design to optimize the ACM as it operates within a larger system. While the results derived through this study provided a basis for optimal control of an aircraft ACM, outside factors were not taken into account that will drive the performance of the ACM. Some of these factors include degradation effects the ACM has on the aircraft engine performance, the thermal demand throughout the entire system not a single cooling demand, and aircraft system performance loss due to ram air flow across the ACM heat exchanger. Further system integration of the ACM with other subsystems will dictate how the control of the TMS architecture for an aircraft should be set up in order to meet all the demands of an aircraft.

7. REFERENCES

[1] T. Mahefkey, K. Yerkes, B. Donovan, and M. L. Ramalingam, "Thermal management challenges for future military aircraft power systems," *SAE Trans.*, vol. 113, no. 1, pp. 1965–1973.

[2] W. J. A. Dahm, "Future Requirements for Thermal Management : Applications and Challenges on the Horizon," 2011.

[3] I. H. Amrhein, M., Wells, J. R., Walters, E. A., Matasso, A. F., Erdman, T. R., Iden, S. M., Lamm, P. L., Page, A. M., and Wong, "Integrated Electrical System Model of a More Electric Aircraft Architecture," in *SAE: Power Systems Conference*, 2008.

[4] J. R. Wells, M. Amrhein, E. A. Walters, S. M. Iden, A. M. Page, P. L. Lamm, and A. F. Matasso, "Electrical Accumulator Unit for the Energy Optimized Aircraft," *SAE Int. J. Aerosp.*, vol. 1, no. 1, pp. 1071–1077, 2008.

[5] A. C. Roberts, R. A., Eastbourn, S. M., and Maser, "Generic Aircraft Thermal Tip-to-Tail Modeling and Simulation," in *47th AIAA/ASME/SAE/ASEE Joint Propulsion Conference & Exhibit*, 2011.

[6] R. A. Roberts and S. M. Eastbourn, "Vehicle Level Tip-to-Tail Modeling of an Aircraft," vol. 17, no. 2, pp. 107–115, 2014.

[7] D. N. Maser, A. C., Garcia, E., and Mavris, "Facilitating the Energy Optimization of Aircraft Propulsion and Thermal Management Systems through Integrated Modeling and Simulation," in *Power Systems Conference*, 2010.

[8] E. Garcia, A. C. Maser, D. N. Mavris, and C. Miller, "INVENT Surrogate Modeling and Optimization of Transient Thermal Responses," in *50th AIAA Aerospace Sciences Meeting*, 2012, vol. 2012–1123.

[9] D. N. Maser, A. C., Garcia, E., and Mavris, "Thermal Management Modeling for Integrated Power Systems in a Transient, Multidisciplinary Environment," in *AIAA/ASME/SAE/ASEE: Joint Propulsion Conference & Exhibit*, 2009.

[10] Z. J. Bodie M., Russell G., McCarthy K. , Lucas E. and W. M., "Thermal Analysis of an Integrated Aircraft Model," *48th AIAA Aerospace Sciences Meeting*. Orlando, 2010.

[11] M. Bodie, "Air Cycle Machine for Transient Model Validation," in *SAE: Thermal Management Ssytems Symposium*, 2016.

[12] J. H. Doty, D. J. Moorhouse, and J. Camberos, "Benefits of Exergy-Based Analysis for Aerospace Engineering Applications: Part 2," in *47th AIAA Aerospace Sciences Meeting*, 2009, no. 2009–1598.

[13] J. H. Doty, D. J. Moorhouse, and J. Camberos, "Benefits of Exergy-Based Analysis for Aerospace Engineering Applications: Part 1," in *46th AIAA*

Aerospace Sciences Meeting, 2008, pp. 2008–4355.

[14] V. Periannan, "Investigation of the Effects of Various Energy and Exergy-Based Objectives / Figures of Merit on the Optimal Design of High Performance Aircraft System," Virginia Polytechnic Institute and State University, 2005.

[15] C. Zaparoli, Edson Luiz, Batista, J., Regina de Andrade, "Numerical Analysis of Typical Aircraft Air-Conditioning," in *20th International Congress of Mechanical Engineering*, 2009.

[16] T. J. Pérez-Grande, I., and Leo, "Optimization of a commercial aircraft environmental control system," *Appl. Therm. Eng.*, vol. 22, pp. 1885–1904, 2002.

[17] S. Zhao, H., Hou, Y., Zhu, Y., Chen, L., and Chen, "Experimental study on the performance of an aircraft environmental control system," *Appl. Therm. Eng.*, vol. 29, pp. 3284–3288, 2009.

[18] T. J. Kotas, "The exergy method of thermal plant analysis." Butterworth Publishers, 1985.

[19] M. D. Griffin, "HOW DO WE FIX SYSTEM ENGINEERING?," in *61st International Astronautical Congress*, 2010, pp. 1–9.

[20] H. Ahamed, J., Saidur, R., Masjuki, "A review on exergy analysis of vapor compression refrigeration system," *Renew. Sustain. Energy Rev.*, vol. 15, no. 3, pp. 1593–1600, 2011.

[21] S. M. Sami, "Energy and exergy analysis of an efficient organic Rankine cycle for low temperature power generation," *Int. J. Ambient Energy*, vol. 29, no. 1, pp. 1–10, 2008.

[22] K. H. Kim, H. J. Ko, and S. W. Kim, "Exergy Analysis of Organic Rankine Cycle with Internal Heat Exchanger," *Int. J. Mater. Mech. Manuf.*, vol. 1, no. 1, pp. 41–45, 2013.

[23] M. Ghazikhani, I. Khazaee, and E. Abdekhodaie, "Exergy analysis of gas turbine with air bottoming cycle," *Energy*, vol. 72, pp. 599–607, 2014.

[24] L. Malinowski and M. Lewandowska, "Analytical model-based energy and exergy analysis of a gas microturbine at part-load operation," *Appl. Therm. Eng.*, vol. 57, no. 1–2, pp. 125–132, 2013.

[25] G. Li, Y. Hwang, R. Radermacher, G. Martin, H. Bldg, and C. Park, "Experimental investigation on energy and exergy performance of adsorption cold storage for space cooling application," *Int. J. Refrig.*, vol. 44, pp. 23–35, 2014.

[26] M. Razmara, M. Maasoumy, M. Shahbakhti, and R. D. R. Iii, "Exergy-Based Model Predictive Control for Building HVAC Systems," 2015.

[27] I. Uckan, T. Yilmaz, E. Hurdogan, and O. Buyukalaca, "Exergy analysis of a novel

configuration of desiccant based evaporative air conditioning system," *Energy Convers. Manag.*, vol. 84, pp. 524–532, 2014.

[28] M. Cengel, Y., Boles, *Thermodynamics: An Engineering Approach*, 6th ed. New York: The McGraw-Hill Companies, Inc., 2008.

[29] J. Vargas and A. Bejan, "Thermodynamic optimization of finned crossflow heat exchangers for aircraft environmental control systems," *Int. J. Heat Fluid Flow*, vol. 22, pp. 657–665, 2001.

[30] N. Jain, "Thermodynamics-Based Optimization and Control of Integrated Energy Systems," University of Illinois, 2013.

[31] M. Hadian, M. H. Asheri, and K. Salahshoor, "A novel exergy-event based model predictive control strategy for energy saving," *J. Nat. Gas Sci. Eng.*, vol. 21, pp. 712–717, 2014.

[32] K. Salahshoor and M. H. Asheri, "A new exergy-based model predictive control methodology for energy assessment and control," *J. Nat. Gas Sci. Eng.*, vol. 21, pp. 489–495, 2014.

[33] G. (Honeywell), "Garrett, Turbocharger Guide Volume 5," 2016.

[34] ConceptsNREC, "COMPAL & RITAL." White River Junction, Vt., 2016.

[35] C. J. Cengel, Y., *Fluid Mechanics*. New York: McGraw-Hill, 2014.

[36] L. A. Kays, W., *Compact Heat Exchangers*. New York: McGraw-Hill, 1984.

[37] W. J. Rugh and J. S. Shamma, "Research on Gain Scheduling," *Automatica*, vol. 36, pp. 1401–1425, 2000.